Computational Analysis of Modified Disk Brake Rotors: Structural and Thermal Characteristics Using ANSYS

[1]Sachin Tripathi [2] Prof. Shamir Daniel

[1]M. Tech Scholar, Department of Thermal Engineering, Truba Institute of Engineering and Information Technology, Bhopal India,

[2]Assistant Professor, Department of Thermal Engineering, Truba Institute of Engineering and Information Technology, Bhopal India,

[1]sachintripathi989@gmail.com, [2]shamirdaniel3004@gmail.com

* Corresponding Author: Sachin Tripathi

Abstract: *This research investigates the structural and thermal characteristics of modified disk brake rotors through computational analysis using ANSYS software. The study aims to compare the performance of a base model with suggested modifications, focusing on safety factor, stress distribution, temperature profiles, heat flux, and deformation. Finite Element Analysis (FEA) is employed to simulate various scenarios and assess the effectiveness of design alterations in enhancing rotor performance. Results show significant improvements in reducing stress levels, heat flux, and thermal gradients, thereby optimizing the braking system's reliability and efficiency.*

Keywords: *Disk brake rotor, ANSYS, structural analysis, thermal analysis, finite element analysis, stress distribution, heat flux, temperature profiles, modal analysis.*

I. INTRODUCTION

The initial law of motion, formulated by the esteemed physicist Sir Isaac Newton, posits that an object will persist in a state of rest or uniform motion in a straight line unless it is subjected to the influence of an external force. The enactment of this legislation precipitated the advancement of braking mechanisms in motor vehicles, necessitating the implementation of an effective braking system and an ample power supply. This event led to a significant scholarly investigation into brake technology and the subsequent development of contemporary braking systems.

The act of braking is an essential and fundamental component of any system that is in motion. It serves a critical purpose in the control of speed, deceleration, and ultimately, the complete cessation of movement. The process under consideration entails the conversion of kinetic energy, which is the energy possessed by an object due to its motion, into various other forms of energy, including but not limited to heat and mechanical work. This conversion mechanism serves the purpose of diminishing the overall motion or movement of the object in question. In the realm of vehicles and machinery, the presence of efficient and reliable braking systems assumes paramount importance in guaranteeing both safety and optimal performance. Throughout history, a plethora of diverse braking mechanisms have been meticulously developed, each possessing its own unique set of principles and applications. These braking mechanisms have played a pivotal role in ensuring the safety and efficiency of various modes of transportation and machinery.

A. Types of Braking

In this detailed discussion, we will explore the different types of braking and their characteristics.

Regenerative Braking

Regenerative braking, a cutting-edge braking technique, has gained widespread adoption in the realm of electric and hybrid vehicles. This innovative approach to braking has revolutionised the way these vehicles operate, offering numerous advantages in terms of energy efficiency and sustainability. By harnessing the power of kinetic energy that is typically dissipated as heat during conventional braking, regenerative braking allows for the recovery and storage of this energy, thereby enhancing on the process involves the utilisation of the kinetic energy generated by the motion of the vehicle, which is subsequently transformed into electrical energy through a conversion mechanism. This electrical energy is then stored in either a battery or a capacitor, enabling its preservation for subsequent utilisation. During the process of regenerative braking, which occurs when the driver disengages the accelerator pedal or activates the braking system, the electric motor undergoes a transition into a generator mode. This mode enables the conversion of the vehicle's kinetic energy into electrical energy. The process plays a crucial role in mitigating the detrimental effects of wear on friction brakes, thereby prolonging their lifespan. Additionally, it serves to enhance the overall range of the vehicle by effectively harnessing and repurposing energy that would otherwise dissipate as heat, resulting in a more efficient utilisation of resources. Regenerative braking has gained recognition for its notable efficiency and environmentally friendly attributes. This innovative braking system enables the recovery of energy that would otherwise be dissipated as heat during braking, thereby reducing the reliance on conventional friction brakes. By harnessing this energy, regenerative braking not only enhances overall efficiency but also contributes to a more sustainable transportation ecosystem.

Hydraulic Braking

Hydraulic braking systems are widely employed in various vehicles and machinery to effectively convert the driver's input into the necessary force to activate the brake mechanisms. These systems rely on the utilisation of fluid pressure as a means of transmitting force throughout the braking system. By harnessing the principles of fluid mechanics, hydraulic braking systems are able to convert the driver's input efficiently and reliably into the required force to engage the brakes. The process involves utilizing hydraulic fluid enclosed within a closed system to transmit the force produced by the driver's input to the brake mechanisms, and thus results in transmitting force. Through the application of fluid pressure, hydraulic braking systems are able to amplify the force exerted by the driver, resulting in a more powerful and responsive braking action. Overall, hydraulic braking systems play a crucial role in ensuring the safety and effectiveness of braking When the driver engages the brake pedal, a mechanical action is initiated whereby a piston within the master cylinder is actuated. This actuation subsequently results in the generation of pressure within the brake fluid, thereby facilitating the transmission of force to the braking system. The pressurised fluid, which serves as a crucial component in the braking system, is subsequently conveyed through brake lines to the wheel cylinders or callipers located at each individual wheel. This transmission of fluid plays a pivotal role in facilitating the effective operation of the braking mechanism. In the context of automotive braking systems, pressure plays a crucial role in facilitating the conversion of kinetic energy into heat energy, thereby enabling the deceleration, or stopping of a vehicle. This process involves the application of force exerted by the brake pads or shoes onto the rotor or drum, resulting in the generation of frictional forces that impede the rotational motion of the wheels. By harnessing the principle of friction, the pressure exerted on the brake components facilitates the conversion of the vehicle's kinetic energy into thermal energy, ultimately leading to the desired braking effect. Hydraulic braking systems have gained significant popularity and widespread adoption in the automotive industry owing to their inherent reliability and highly responsive operation. These systems have emerged as a preferred choice for vehicle manufacturers and consumers alike, owing to their ability to effectively convert mechanical force into hydraulic pressure, thereby facilitating efficient and controlled deceleration of the vehicle. The reliability of hydraulic braking systems stems from their robust design and construction. These systems are engineered to withstand the demanding conditions encountered during vehicle operation, including extreme temperatures, varying road surfaces, and heavy loads. By employing high-quality materials and precise manufacturing techniques, hydraulic braking systems are able to deliver consistent and dependable performance, ensuring the safety and confidence of drivers and passengers. Furthermore, the One of the key functions of mechanical brakes is to offer a substantial mechanical advantage, thereby enabling the driver to exert a relatively minimal force on the brake pedal while generating a substantial braking force at the wheels. This mechanical advantage is crucial in facilitating effective braking mechanisms in various vehicles.

Electromagnetic Braking

Electromagnetic braking is a braking mechanism that operates based on the fundamental principle of electromagnetic force. This braking system utilises the force generated by electromagnetic fields to produce the necessary braking action. The utilisation of this technology is prevalent in various applications, including but not limited to lifts, trains, and certain types of industrial machinery. Electromagnetic brakes are composed of two main components: a fixed coil and a rotating armature or rotor. This design allows for efficient conversion of electrical energy into mechanical braking force. The stationary coil, also known as the stator, is responsible for generating a magnetic field when an electric current pass through it. On the other hand, the rotating armature, or rotor, is connected to the braking mechanism and is subjected to the magnetic field produced by the coil. As a result, when an electric current is introduced to the coil, a magnetic field is generated, which in turn exerts an attractive force on the armature. This attractive force ultimately leads to the initiation of the braking action. The adjustment of the braking force can be achieved through the manipulation of the electric current. By exerting control over the flow of electric current, the braking force can be finely tuned and regulated to meet specific requirements. This capability to modulate the braking force through the manipulation of electric current provides a versatile and adaptable means of achieving optimal braking performance in various contexts and scenarios. The utilisation of electromagnetic braking systems presents a multitude of advantages in various applications due to its ability to offer precise control, rapid response, and the flexibility to provide either continuous or intermittent braking. This technology has proven to be highly advantageous in numerous industries, including automotive, aerospace, and industrial sectors. By harnessing the power of electromagnetic forces, these braking systems enable enhanced control over braking operations, ensuring optimal performance and safety. The quick response time of electromagnetic braking systems allows for swift deceleration, contributing to improved efficiency and reduced stopping distances. Furthermore, the ability to adjust the braking force continuously or intermittently based on the specific requirements of the application further enhances the versatility and adaptability of electromagnetic braking systems.

Aerodynamic Braking

Aerodynamic braking serves as a crucial mechanism employed in aircraft operations to effectively decelerate the aircraft during the landing phase, thereby facilitating a reduction in the ground roll subsequent to touchdown. The process of reducing an aircraft's speed involves the strategic deployment of specialised aerodynamic devices, such as spoilers or airbrakes. These devices are designed to increase the drag experienced by the aircraft, thereby facilitating a decrease in its velocity. By manipulating the airflow around the aircraft, spoilers and airbrakes effectively counteract the forward momentum, resulting in a reduction of speed. This technique is commonly employed in aviation to ensure safe and controlled deceleration during various flight phases, such as landing or approach. These devices, known as aerodynamic

spoilers or airbrakes, serve the purpose of augmenting the surface area or altering the airflow patterns over the wings of an aircraft. By doing so, they effectively generate drag forces that act in opposition to the aircraft's forward motion, thereby aiding in the process of deceleration or reducing the speed of the aircraft. Aerodynamic braking contributes to improved handling and shorter landing distances by increasing drag.

Dynamic Braking

Dynamic braking is a widely utilised technique in various applications, particularly in the realm of electric trains and electric motors, where the rapid dissipation of energy is of paramount importance. This braking method is specifically designed to efficiently transforms the kinetic energy of the moving system into electrical energy, thereby enabling the dissipation of excess energy in a swift and controlled manner. By harnessing the principles of electromagnetic induction, dynamic braking effectively transforms the mechanical energy of the system into electrical energy, which can then be dissipated through resistive elements or fed back into the power supply system. This approach not only ensures the prompt deceleration of the system but also facilitates the recovery and reuse of the dissipated energy, thereby enhancing overall energy efficiency. Consequently, dynamic braking has emerged as a crucial component in the design and operation of electric trains and electric motors, enabling them to achieve optimal performance and energy management. The braking system in question effectively employs the inherent windings of the motor as a resistor for the purpose of deceleration. During the deceleration phase or when functioning as a generator, the motor produces electrical energy which is subsequently dissipated as heat through the utilisation of a resistor or a grid of resistors. This dissipation process helps to manage and regulate the excess energy generated by the motor, thereby preventing any potential damage or malfunction. The process of energy dissipation plays a crucial role in generating a braking effect, thereby effectively reducing the velocity of the motor or vehicle. Dynamic braking is a highly effective method that can be employed in various scenarios where conventional friction brakes may prove inadequate or when the recovery of energy is not a primary concern. By harnessing the power of electromagnetic forces, dynamic braking offers a viable alternative to traditional braking systems in situations where additional stopping power is required or when the dissipation of excess kinetic energy is necessary.

Friction Braking

Friction braking, which is widely recognized as the most prevalent and extensively employed technique for deceleration in various modes of transportation, holds a prominent position in the field of vehicle braking systems. The underlying mechanism of this process is predicated upon the fundamental principle of transforming kinetic energy into thermal energy by means of the frictional interaction that occurs between two surfaces. Within the context of this particular mechanical process, it is observed that brake pads or shoes, which are typically composed of friction materials such as composite materials or ceramics, are effectively applied against a rotating surface, commonly referred to as the rotor or drum. The primary objective of this action is to generate frictional forces that effectively impede or halt the rotational motion. The process of frictional interaction involves the conversion of kinetic energy possessed by a moving system into heat energy, resulting in its dissipation into the surrounding environment. This phenomenon occurs due to the resistance encountered by the moving system as it comes into contact with its surrounding surfaces. As a result of this interaction, the kinetic energy of the system is gradually converted into thermal energy, leading to the dissipation of heat into the surrounding environment. Friction braking is a widely utilised mechanism in a diverse range of applications, encompassing automotive vehicles, trains, bicycles, and industrial machinery. This braking technique relies on the principle of friction to transform kinetic energy into thermal energy, thereby facilitating the deceleration or complete halt of the respective systems. In the realm of automotive vehicles, friction braking plays a pivotal role in ensuring safe and controlled stopping, enabling drivers to effectively manage their speed and navigate through traffic.

B. Disk and Drum Brakes

They are two different types of braking mechanisms that utilize frictional contact to slow down or stop the motion of vehicles. Let's explore each of them in detail:

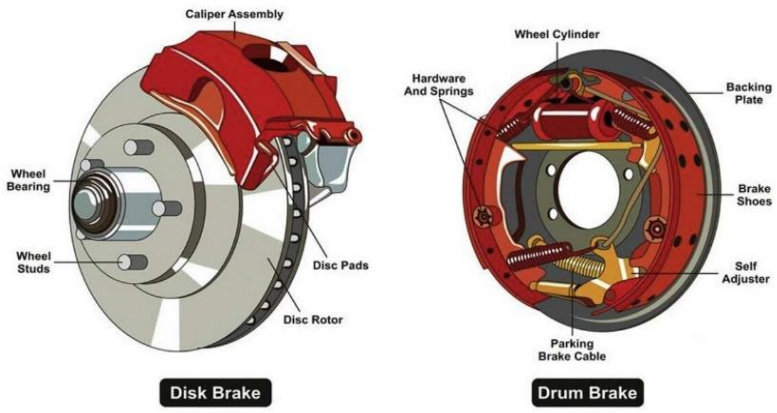

Fig. 1.1 Disk and Drum Brakes

Drum Brakes

Drum brakes, on the other hand, use frictional contact between brake shoes and the inner surface of a drum to generate braking force. Here are some key characteristics of drum brakes:

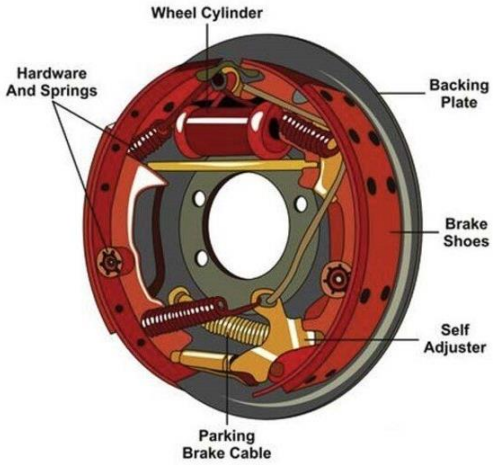

Fig. 1.2 Drum Brakes

Components: Drum brakes consist of a brake drum, brake shoes, and a wheel cylinder that pushes the brake shoes against the inner surface of the drum.

Fig. 1.3 Drum brakes consist of a brake drum

Mechanism: When the brakes are applied, hydraulic pressure is exerted on the wheel cylinder, causing the brake shoes to engage against the inner lining of the drum. The frictional interaction between the layer of brake shoes and the wall of drum generates the braking force, resulting in halting or stopping of the vehicle.

Advantages: Drum brakes are typically less expensive and simpler in design compared to disc brakes. They are also more resistant to environmental elements such as dirt, water, and debris. Drum brakes tend to be more effective at parking and holding a vehicle stationary

Each braking system has its own advantages and limitations, and their suitability depends on various factors including vehicle type, application, and desired performance. In modern vehicles, disc brakes are commonly used on the front wheels, while drum brakes may be utilized on the rear wheels. The combination of both types provides a balanced braking system that optimizes performance and safety.

Disc Brakes

Disc brakes operate by pressing brake pads against a rotating metal disc (rotor) attached to the wheel or axle. The frictional contact between the brake pads and the disc generates the necessary braking force. Here are some key characteristics of disc brakes:

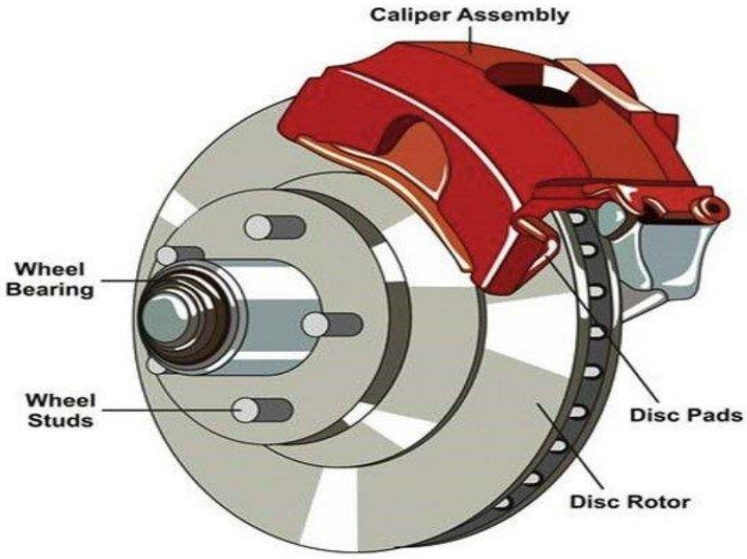

Fig. 1.4 Disc Brakes

Components: Disc brakes consist of a brake disc (rotor), brake pads, and a calliper that houses the brake pads. The calliper applies hydraulic pressure to push the brake pads onto the disc.

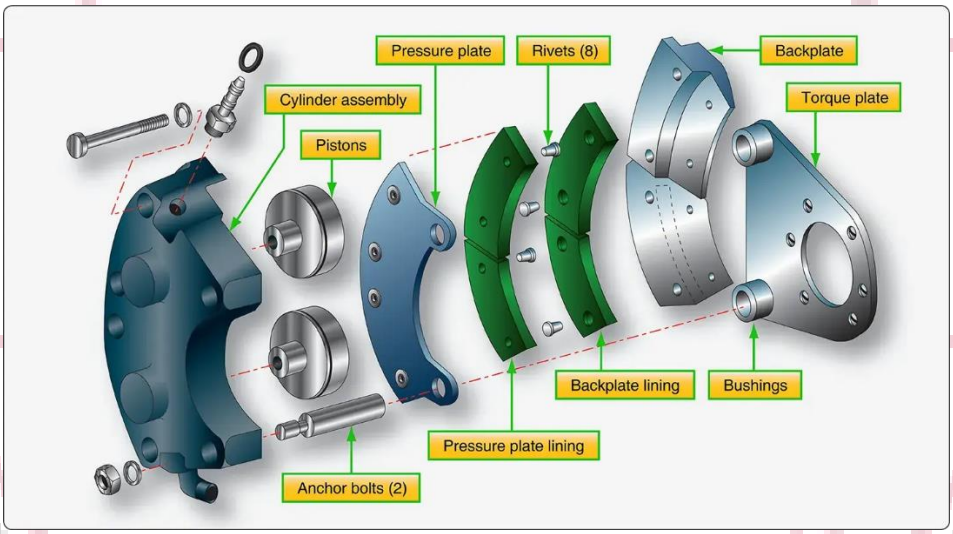

Fig. 1.5 Diagram of Clutch Parts

Mechanism: When the brakes are applied, hydraulic pressure is exerted on the calliper, causing the brake pads to squeeze against the rotating disc. This generates frictional forces that slow down or stop the rotation of the disc, resulting in deceleration or stopping of the vehicle.

Advantages: Disc brakes offer efficient heat dissipation due to their exposed design, which helps in reducing the risk of brake fade. They provide reliable and consistent braking performance, even under heavy braking conditions. Disc brakes are generally easier to service and maintain, and they tend to have shorter stopping distances compared to drum brakes

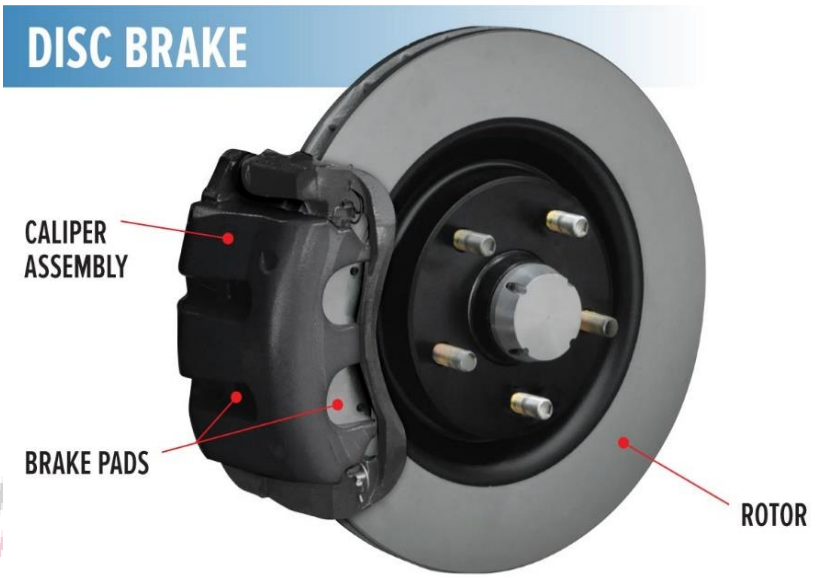

Fig. 1.6 Components are integral parts of a disc brake system

II. LITERATURE REVIEW

Adamowicz, A., & Grzes, P. (2011) This study employs both two- and three-dimensional finite element modeling techniques to investigate temperature distributions resulting from the sliding interaction between components in a disc brake system. Initially assuming a simplified model with uniform heat flux, they transition to a more realistic three-dimensional model incorporating non-axisymmetric thermal loads. The research analyzes the impact of operational parameters and material properties on temperature evolution during braking, emphasizing significant non-uniform temperature distributions within the rotor during emergency braking. The findings validate the effectiveness of advanced modeling in capturing complex thermal behaviors in brake systems.

Vdovin, A. et al. (2020) The paper reviews the traditional and emerging simulation techniques used in brake system design to optimize heat dissipation and prevent brake overheating. It discusses the challenges and limitations of virtual testing compared to physical experiments, highlighting the complexities involved in accurately simulating brake cooling processes. The study consolidates various methodologies and their capabilities in simulating brake system performance across different loading conditions, providing insights into the transition towards simulation-driven design in vehicle manufacturing.

Biradar, D. et al. (2014) This review covers computational and experimental analyses over the past two decades concerning thermal properties of disc brake rotors. It explores advancements in heat conduction, convection, and radiation theories, emphasizing the role of computational methods in deriving engineering solutions for brake systems. The paper underscores the benefits of computational models in addressing the transient nature of braking systems, offering straightforward engineering relationships crucial for understanding thermal dynamics.

Tripathi, V. K., et al. (2023) Focused on the structural analysis and material selection for disc brake rotors, this review explores the use of alternative materials such as Titanium, Magnesium Alloy, Aluminum Alloy, and Structural Steel. Utilizing CATIA for modeling and ANSYS Workbench for structural analysis, the study compares these materials with traditional Grey Cast Iron, aiming to optimize the design of ventilated disc brakes. It provides insights into enhancing braking efficiency and safety through advanced material exploration and analysis.

Thakre, S., et al. (2021) This comprehensive review examines various ventilation patterns and their impact on the thermal and structural performance of disc brake systems. It highlights the importance of designing discs with optimal thermal characteristics to improve braking efficiency without compromising strength. The paper identifies research gaps and proposes thermo-mechanical analyses to optimize disc brake performance through temperature and weight reduction strategies.

Mulani, S. M. et al. (2022) Focusing on tribological aspects, this review addresses abrasive and adhesive wear mechanisms in brake pad-disc systems, particularly the environmental impact of wear debris. It discusses the material properties of conventional brake disc materials like grey cast iron and their susceptibility to wear and corrosion. The study underscores the significant role of friction material selection in determining braking performance under diverse conditions, essential for enhancing automotive safety.

Rahimi, M. et al. (2021) This review consolidates research on airborne wear debris generated by brake systems, emphasizing experimental methodologies for sampling and characterizing brake wear particles. It categorizes studies into subsystem, system, and environmental-level analyses, highlighting the variability in experimental outcomes and the

importance of simulation in interpreting these findings. The paper advocates for bridging gaps between experimental and simulation approaches to advance understanding and mitigation of airborne brake wear emissions.

Ilie, F. et al. (2022) Focused on the friction and wear behavior of materials used in disc-pad braking systems, this paper examines how structural modifications impact system stability and reliability. It evaluates frictional properties, wear patterns, and friction coefficients using dedicated testing methods to enhance braking system design and performance predictions through computer simulations. The findings contribute valuable insights into optimizing disc-pad couples for improved braking efficiency and reliability.

Chand, G. G. et al. (2019) This review explores the thermal response and structural integrity of disc brakes under braking conditions using Finite Element Analysis (FEA) and analytical methods. It compares the performance and lifespan of disc brakes made from different materials such as cast iron, aluminum metal matrix composites (ALMMC), and steel. The study underscores the critical role of heat dissipation in maintaining disc brake efficiency and safety across various operating conditions.

Prabith, K. et al. (2020) Investigating the historical evolution of brake systems, this review highlights advancements that have enhanced vehicle safety and reduced accidents. It traces the development of automotive brakes over four decades, focusing on technological innovations aimed at improving braking efficiency and safety through various design improvements and innovative technologies.

III. OBJECTIVES

- To investigate the structural and thermal characteristics of modified disk brake rotors through computational analysis using ANSYS.
- To compare the features of the suggested model, the modified model, and the base model.
- To perform modal analyses on the disk rotors to determine the peak harmonic frequencies.
- To calculate the values of five criteria: safety factor, equivalent stress, temperature, heat flux, and deformation.

IV. METHODOLOGY

Further elucidation regarding the research philosophy is presented herein. This section focuses on the research conducted, which involves several steps. Firstly, a disc brake prototype was developed using ANSYS software, incorporating certain design modifications. Subsequently, the rotor material was chosen based on its properties and suitability for use as disc. Theoretical calculations were then performed using an energy-saving methodology, specifically tailored to the properties of the front disc brake. Finally, the obtained results were compared with quantitative data.

A. The Application of Finite Element Analysis (FEA)

In order to address intricate engineering challenges, three primary methodologies are commonly employed: analytical methods, experimental methods, and numerical methods. While analytical approaches provide accurate solutions, their applicability is limited to straightforward geometries. Experimental methodologies have the capacity to yield outcomes of high precision; however, their implementation often incurs substantial costs, rendering them economically unfeasible in many instances. The finite element analysis (FEA) approach is a versatile and comprehensive numerical tool that can effectively address engineering challenges through numerical solutions. The process of dividing a given domain into a set of simple subdomains referred to as finite elements is a fundamental aspect of Finite Element Analysis (FEA). The accuracy of the modelling and subsequent analysis increases proportionally with the number of finite elements employed. The finite element method is a numerical approach that is specifically designed to effectively solve differential equations.

A differential equation is the term used to describe any equation involving derivatives, whether they are ordinary or partial. The potential classifications of these entities include linear, partial, or regular. Differential equations hold considerable importance within the realm of environmental studies due to their role as a formal means of expressing the fundamental principles governing physical phenomena. The objective of finite element analysis (FEA) is to transform the differential equations of a given system into a set of linear equations, thereby enabling their solution using computer software.

B. The Ansys Software

The process of addressing nonlinear equations typically involves three fundamental stages: formulation of a mathematical model, resolution of the problem, and examination of the resulting outcomes. Similar to other finite element analysis (FEA) systems, Ansys consists of three main components: the pre-processor, solution processor, and post-processor. These components, namely the processors, play a crucial role in the functioning of Ansys.

The Ansys pre-processor allows users to generate topology, specify materials, and create element meshes. The Ansys processor enables users to apply various loads to problem scenarios in order to derive solutions. The Ansys post-processor facilitates the presentation of tabulated results and the visualisation of data, as well as the generation of hardcopies.

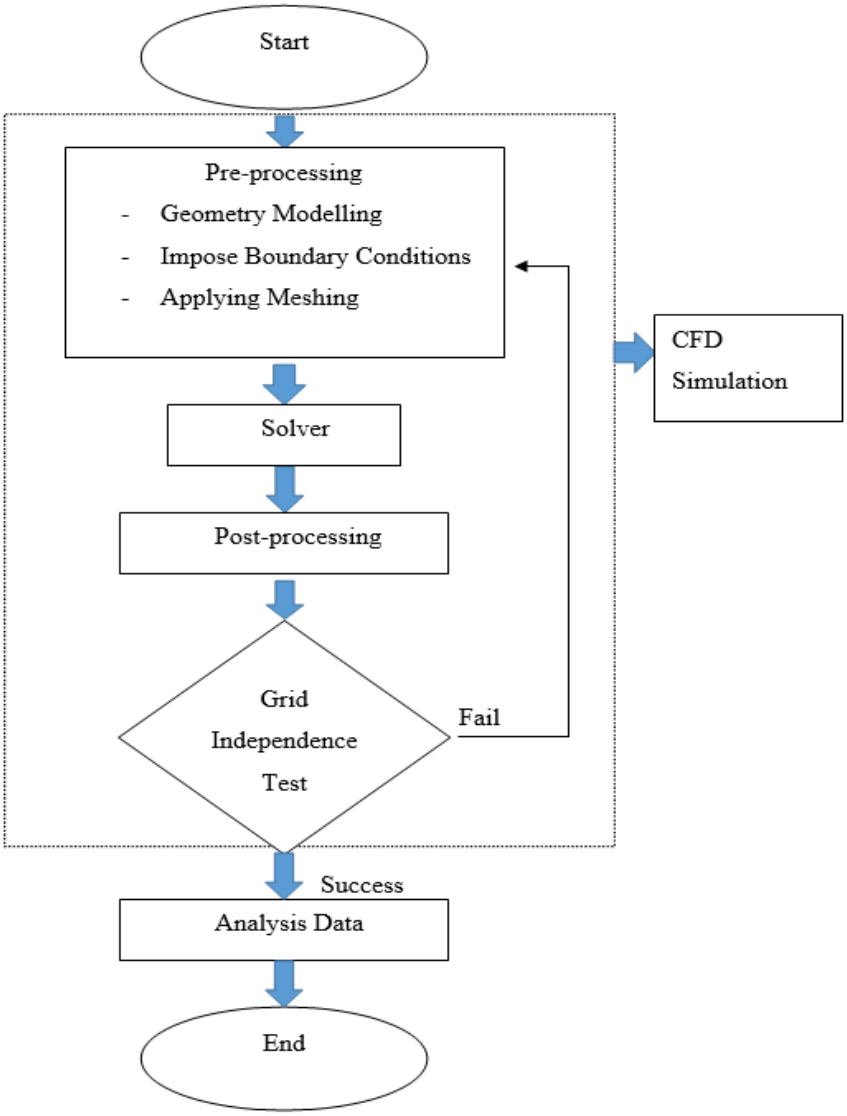

Fig. 4.1 Working Steps of ANSYS software

The comprehensive software suite offered by Ansys enables the design process to incorporate a wide range of engineering simulations, thereby encompassing various domains of study within the field of engineering. This suite effectively encompasses the entire spectrum of physics. Companies worldwide depend on Ansys to optimise their return on investment in engineering simulation software.

The challenge of incorporating diverse elements into a system to guarantee their intended functionality becomes more pronounced as the complexity of products escalates. Ansys finds application in various domains such as computer modelling, industrial sectors, tooling, as well as automotive and aerospace design. Ansys is widely utilised in various applications where Finite Element Analysis (FEA) is employed. The tool under consideration possesses significant efficacy and a multitude of capabilities due to its longstanding dedication to Finite Element Analysis (FEA) applications.

C. Braking Energy and Power

Braking Energy

Fc ter speed V1 to a lesser speed V2, the braking energy E_{flat} is –

$$E_{flat} = \frac{M\,(V1^2 - V2^2)}{2} + \frac{I\,(\alpha 1^2 - \alpha 2^2)}{2} \quad (4.1)$$

Here, V1 and V2 are Initial and Final Velocity and

α1 and α2 are Initial and Final angular velocity.

M stands for Mass of the vehicle

I stands for the rotating pieces' mass moments of inertia.

If the vehicle slows down to stop, then V2= α2 =0 and Equation 4.1 becomes

$$E_{flat} = \frac{M\,(V1^2)}{2} + \frac{I\,(\alpha 1^2)}{2} \quad (4.2)$$

We know that, V= αr

Here "r" is the radius of the wheel, then Equation 4.2 becomes

$$E_{flat} = \frac{M}{2}\left(1 + \frac{I}{r^2 M}\right)V1^2 = \frac{cMV1^2}{2} \quad (4.3)$$

In above Equation, $\frac{I}{r^2 M} = c$; that is correction factor of rotating masses

Braking Power

The rate at which the mechanical energy changes in relation to time t is known as the braking power, or

$$P_{flat} = \frac{d\,(Energy)}{dt} \quad (4.4)$$

The definition of velocity V can be written as follows if "a" denotes the decelerate and its value is constant;

$$V(t) = V1 - at \quad (4.5)$$

By using Equation (4.4) and Equation (4.5), instantaneous power will be calculated as –

$$P_{flat} = cMa\,(V1 - at) \quad (4.6)$$

The vehicle pauses when the braking force is at its lowest and is at its greatest when time (t) = 0, according to Eq. (4.6). As a result, the braking power fluctuates during the braking period, peaking at the start of braking and then progressively decreasing until it drops to zero.

D. Convection Heat Transfer Coefficient

The convective heat transfer coefficient, which varies depending on the vehicle's speed, construction, and placement of the braking elements, is crucial information for calculating the temperature of the brakes. In many circumstances, determining the heat transfer coefficient at an average speed is sufficient. The brakes are additionally cooled by radiation as well as conduction. However, conduction only redistributes heat, which affects temperature and may put other crucial components like bearings, lubricants, or sealants in danger.

It's crucial to remember that any heat transfer coefficient equation can only yield approximations. The cooling is demonstrated by the following formulae:

$$Nu = H.Re^m.Pr^n \quad (4.7)$$

Here we know that,

H denotes the ***Heat Transfer Coefficient***;

Re denotes the ***Reynolds Number***;

Pr denoted the ***Prandtl Number***;

Nu denotes the ***Nusselet Number***.

After looking at Equation (4.7), let's examine the methods for determining the Nusselt Number, Reynolds Number, and Prandtl Number in turn.

When computing the Nusselt number in Equation (4.8), keep in mind that,

$$\text{Nusselet Number } (Nu) = \frac{H_c(r/2)}{T_a} \quad (4.8)$$

"Hc," "r," and "Ta" are used to indicate the convection heat transfer coefficient, outer radius of the disc, and air's electrical properties, respectively.

$$\text{Reynolds Number } Re) = \frac{\rho\, S\,(r/2)}{\nu_a} \quad (4.9)$$

When computing the Reynolds number in Equation (4.9), keep in mind that,

The outer radius of the disc is denoted by "r," the vehicle's speed is denoted by "S," and the kinematic viscosity of the air is indicated by "va." The density of the air is denoted by " ρ"

Prandtl Number $(Pr) = \frac{3600\, S_h\, M}{T_a}$ (4.10

When calculating the Prandtl in Equation (4.10), keep in mind that,

Specific Air's heat is denoted by "Sh," its mass flow rate is denoted by "M," and its thermal conductivity is shown by "Ta."

Depending on how the brake is set up, the constant "H" has a different value for brake drums, solid rotors, and ventilated rotors. The heat transfer variable m is impacted by the flow pattern, such as turbulent, laminar, or transitional flow. The heat transmission variable n is governed by the properties of the flowing air.

E. Analytical Method for Temperature Analysis

The heat generated by friction on both surfaces heats conduction, which heats the solid, non-ventilated rotor employed in the evaluation. An analytical thermometer solution using constant heat flow is given below as an equation for these conditions.

$$\phi_0(z,t) = \frac{Q_0}{H_c}\left(2\frac{\phi_i H_c}{Q_0} - 1\right)\sum_{n=1}^{\infty} \frac{\sin(\Upsilon_n T_{1/2})}{(\Upsilon_n T_{1/2}) + \cos(\Upsilon_n T_{1/2})\sin(\Upsilon_n T_{1/2})} e^{-a_t(\Upsilon_n{}^2 T)} cos(\Upsilon_n D) + 1 \quad (4.11)$$

Variables in the equation above can be expressed as,

Brake's relative temperature as a result of a continuous heat flux is 0;

Initial temperature difference between brake and ambient = ϕ_i;

Average heat flux into rotor = Q_0;

$T_{(1/2)}$ =one-half rotor thickness;

D= horizontal distance measured from mid-plane of rotor;

Υ_n= nΠ/$(T_{1/2})$

The aforementioned equation determines the temperature response for a constant heat flux at the base of the rotor. But as the car slows down, the heat flux evolves over time. Calculating the temperature while using a linearly decreasing heat flux requires the use of the aforementioned formula, the Duhamel theorem, or aggregation integral.

F. Methodological Approach

The brake mechanism in automobiles is a critical component that ensures functionality and safety. To enhance braking performance, it is crucial to have a well-designed rotor and effective heat dissipation material. This study aims to analyze the stress and temperature distribution in a modified ventilated disc brake rotor. The modified rotor incorporates curved vents, holes, and slots. The objective is to achieve a low-stress state prior to engaging the brake, while also considering the insignificance of inertia and body force effects.

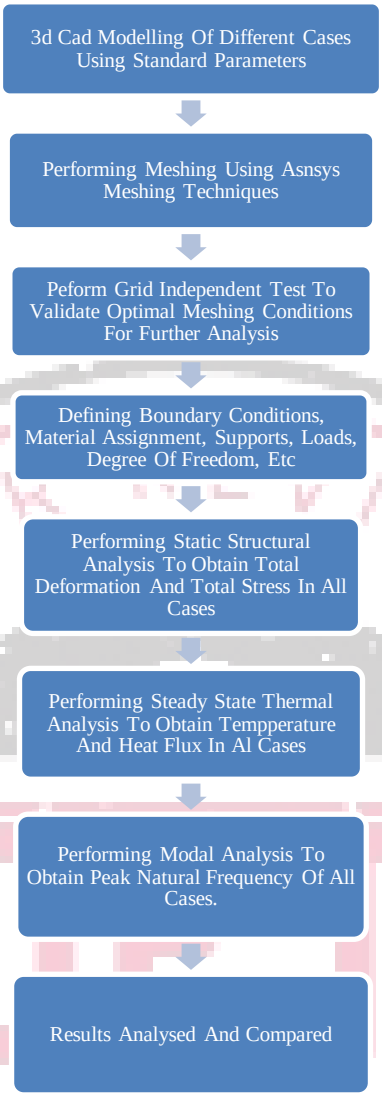

Fig. 4.2 Framework of the proposed methodology

The research methodology consists of four cases: the base model and three modified models. Each case undergoes several analyses, including Static Structural Analysis, Steady State Thermal Analysis, and Modal Analysis. These analyses provide insights into key parameters such as Total Deformation, Modal Frequencies, Heat Flux, Equivalent Stress, Meshing, and Temperature.

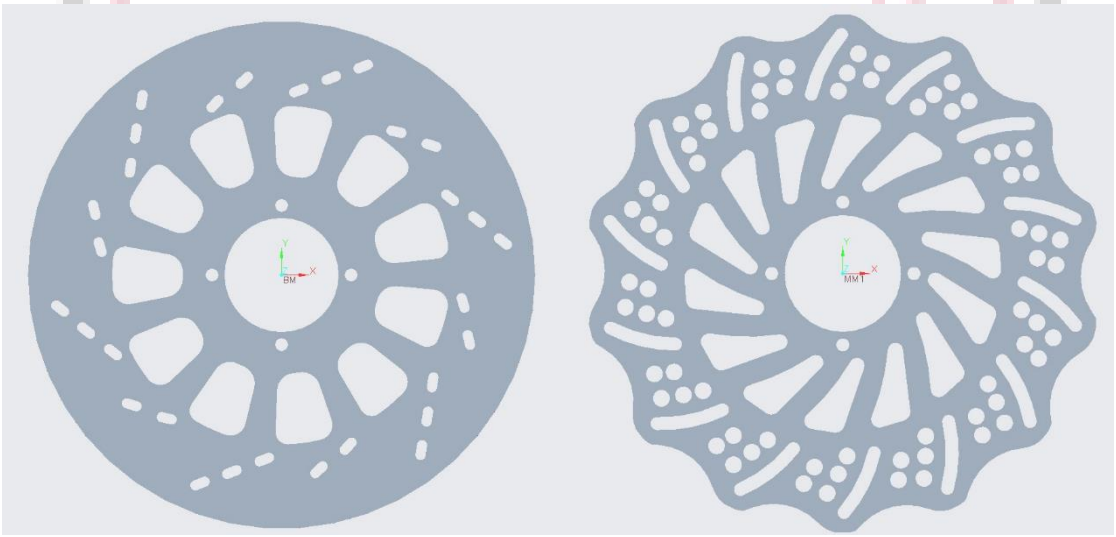

Base Model **Case 1**

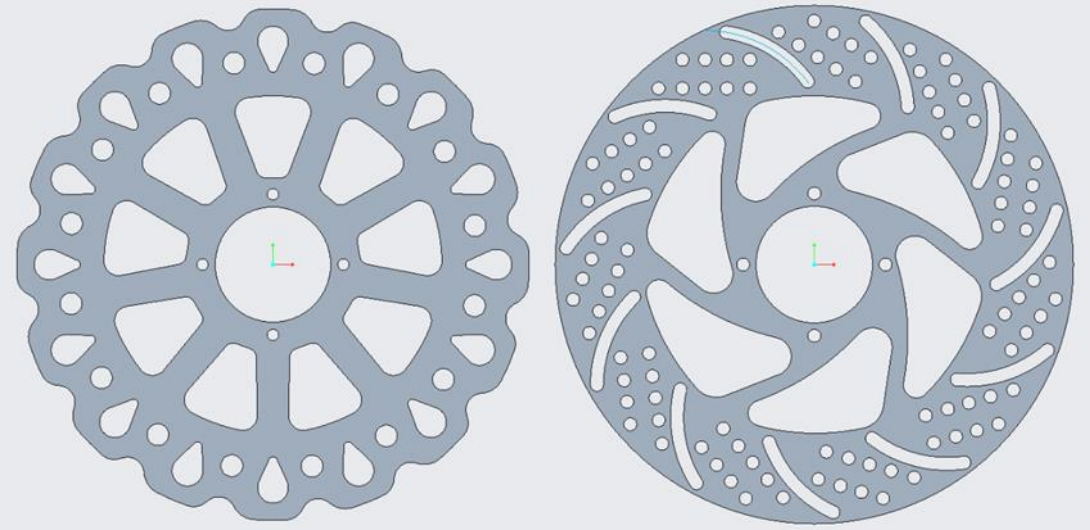

Case 2 **Case 3**

Fig. 4.3 Methodology: 3 Cases - Base & Modified Models

Table 4.1 Key Features Utilised for Model Generation

Feature	Details
Outer diameter	200 mm
Inner diameter	150 mm
Thickness	3.5 mm
Brake pad surface (area)	35mm (3848.45 mm²)
Wheel hub support	4
Material (yield strength)	Stainless steel (207MPa)
Co-efficient of friction	0.5
Maximum pressure applied	1MPa

CAD models of all the cases were prepared using PTC Creo parametric software, four cases are made, and material assigned to all cases remains the same for all the cases i.e., structural steel.

here is a tabular representation of various material properties of structural steel typically used in ANSYS for structural, modal, and thermal analysis:

Table 4.2 Material Properties of Structural Steel

Property	Value (Typical for Structural Steel)
Young's Modulus (E)	200 GPa (29,000 ksi)
Poisson's Ratio (ν)	0.3
Density (ρ)	7850 kg/m³ (489 lb/ft³)
Thermal Conductivity (k)	45 W/m·K (26 BTU/(hr·ft·°F))
Specific Heat Capacity (Cp)	490 J/kg·K (0.117 BTU/(lb·°F))
Coefficient of Thermal Expansion (α)	12 x 10^-6 /°C (6.67 x 10^-6 /°F)
Yield Strength (σy)	250 MPa (36,000 psi)
Ultimate Tensile Strength (σu)	400 MPa (58,000 psi)
Thermal Diffusivity (α)	11.6 x 10^-6 m²/s (4.33 x 10^-5 in²/s)

Meshing: A diagram depicting the mesh structure used for the analysis, showing how the model is discretized into smaller elements for computational purposes.

Meshing Strategy

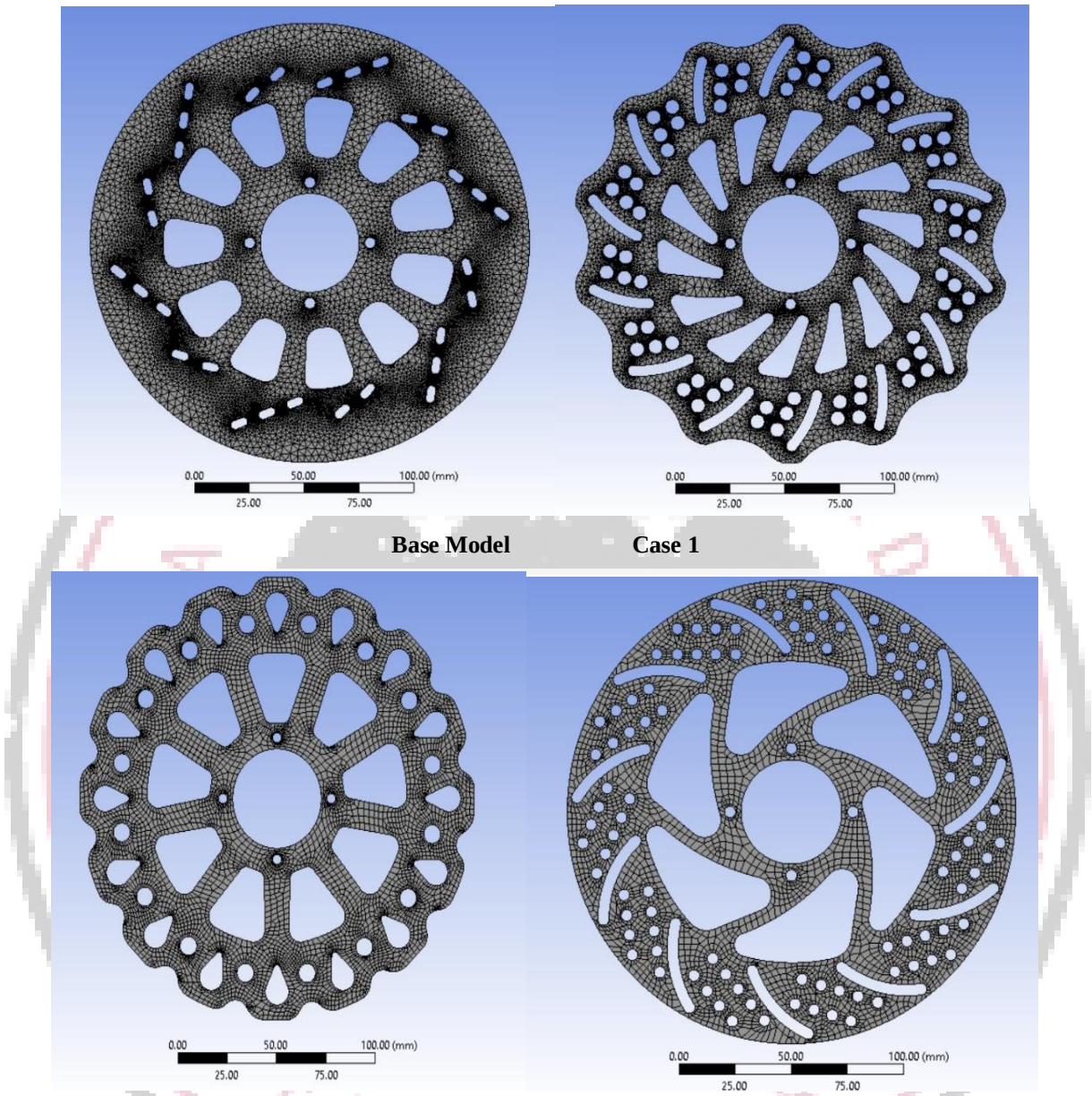

Fig. 4.4 Meshing Strategy of all cases

The meshing process is a critical step in numerical simulations as it involves discretizing the complex geometry of the disk brake motor into smaller elements to facilitate computational analysis. In this study, a high-resolution meshing approach was employed, using a default smoother level of 0.050000 and a goal quality of 0.050000. The primary objective of this strategy is to create a finely detailed mesh that accurately represents the intricate features of the disk brake motor, ensuring that the subsequent analysis yields reliable results.

To further enhance the mesh quality and capture smooth transition regions, the gradual transition inflation option was utilized. This option allows for a controlled transition between different mesh sizes, reducing potential numerical artefacts that could arise from abrupt changes in mesh resolution. The transition ratio of 0.272, which is set to its default value, ensures a seamless progression of the mesh, enhancing accuracy in regions where gradients and abrupt changes occur.

The redesigned model, while maintaining similarity with the original model, underwent mesh refinement, resulting in 435286 elements and 657513 nodes. This process ensured that the model remained computationally efficient while preserving the accuracy of the analysis. The significance of mesh refinement lies in its ability to capture localized phenomena and fine features, which may not be adequately represented by a coarser mesh.

Grid Independent Test

To evaluate the computational accuracy and assess the mesh's sensitivity to grid resolution, a grid-independent test was conducted. For this purpose, three distinct mesh styles were selected: coarse, medium, and fine. These mesh styles were specifically chosen to investigate the effect of varying mesh resolution on the simulation results.

During the grid-independent test, simulations were run using each mesh style, and the results obtained were compared against one another. The goal of this analysis was to identify the level of mesh refinement required to achieve convergence and consistency in the simulation results. Convergence, in this context, refers to the attainment of consistent and repeatable results as the mesh is further refined, indicating that the solution is independent of the mesh size.

Table 4.3 Grid Independent Test Performed on Ansys

Property	Coarse	Medium	Fine
No. of elements	6478	11202	464639
Temperature (°C)	51.603	51.605	51.604
Heat flux (W/m²)	0.19885	0.14478	0.13732
Equivalent stress (MPa)	100.33	103.22	103.16
Deformation (mm)	0.035124	0.035069	0.035044

By comparing the results obtained from each mesh style, it was observed that the finer mesh styles (medium and fine) exhibited convergence, indicating that the results were consistent and independent of the mesh resolution. On the other hand, the coarse mesh style yielded results that deviated significantly from those of the finer meshes, suggesting a lack of convergence and reduced accuracy.

Based on the grid-independent test, it was determined that the fine mesh style strikes a suitable balance between computational efficiency and accuracy. While the fine mesh demands greater computational resources, it ensures highly precise and reliable results, making it the preferred choice for this analysis.

In summary, the meshing strategy employed in this study focused on creating a high-resolution mesh with gradual transition inflation to accurately represent the intricate geometry of the disk brake motor. The mesh refinement process, while preserving computational efficiency, enabled the analysis to capture critical features and localized phenomena.

The grid-independent test reaffirmed the significance of mesh resolution, with the fine mesh style proving to be the most appropriate choice for achieving convergence and accurate results. This study's findings emphasize the importance of meshing in numerical simulations and provide valuable insights into optimizing computational efficiency while maintaining accuracy in the analysis of complex mechanical systems like the disk brake motor.

G. Results for Static Structural analysis compiled after performing on all cases

Total Deformation: This analysis determines the extent of deformation that occurs in the base model when subjected to applied loads. It helps assess how the model responds and deforms under different stress conditions.

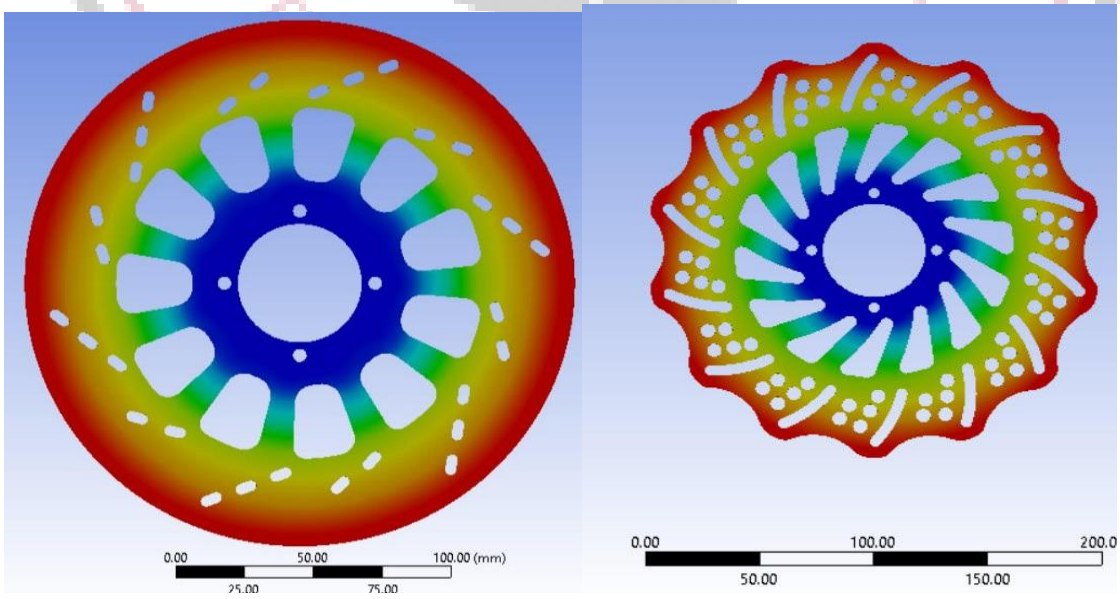

Base Model **Case 1**

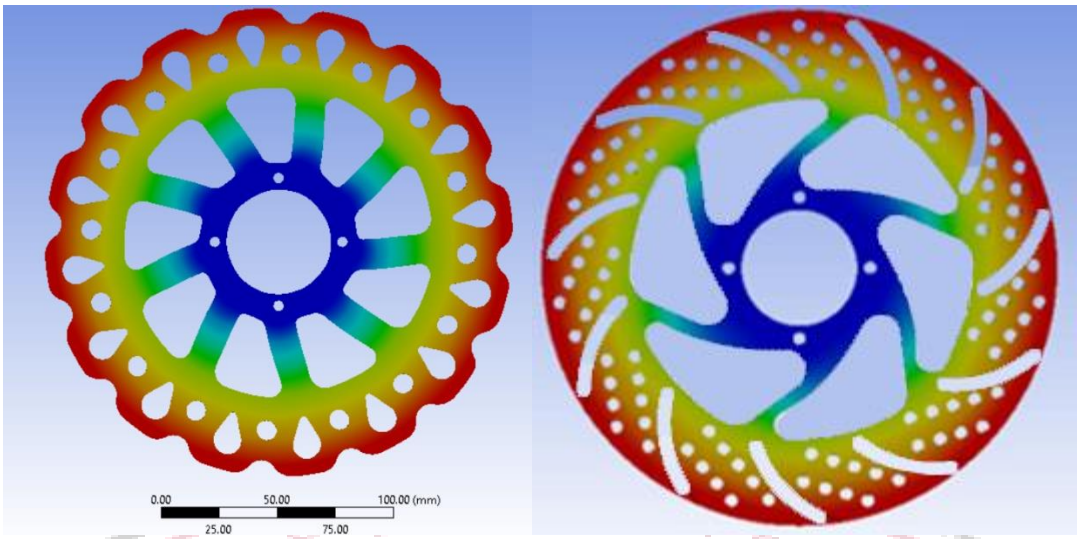

Case 2 **Case 3**

Fig. 4.5 Total Deformation of all cases

Equivalent Stress: Equivalent Stress: The distribution of stress across the base model is analyzed to ensure that it remains within acceptable limits and to evaluate the structural integrity of the model.

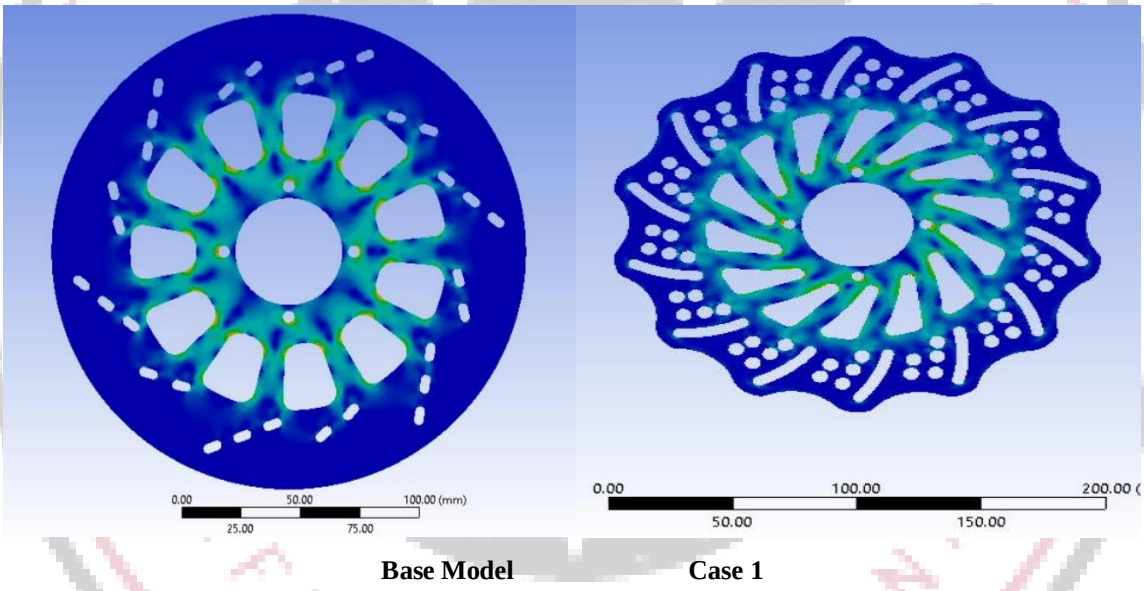

Base Model **Case 1**

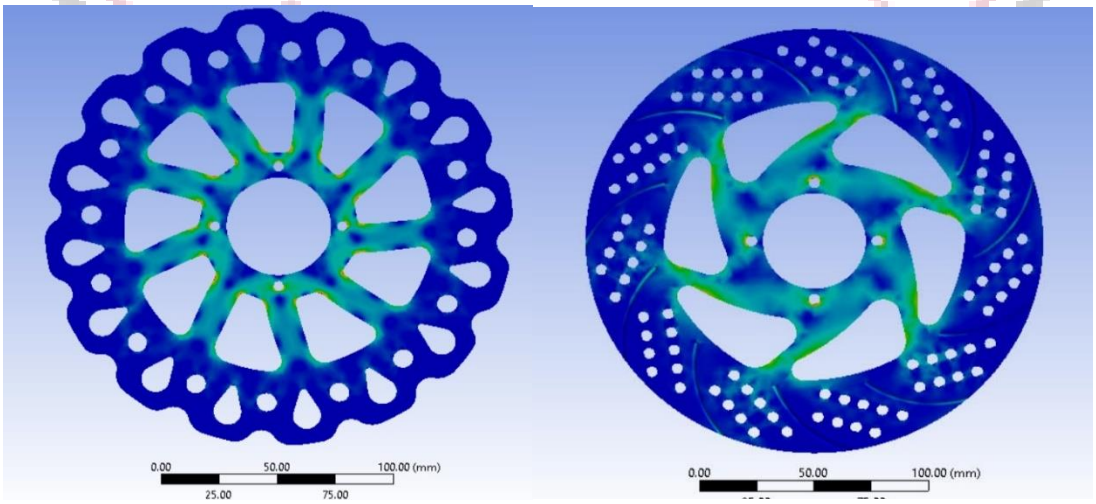

Case 2 **Case 3**

Fig. 4.6 Equivalent stress of all cases

H. Results for Steady State Thermal analysis compiled after performing on all cases

Heat Flux: This analysis focuses on measuring the heat dissipation capabilities of the base model. It helps understand how heat is transferred and distributed within the model, providing insights into its thermal behaviour.

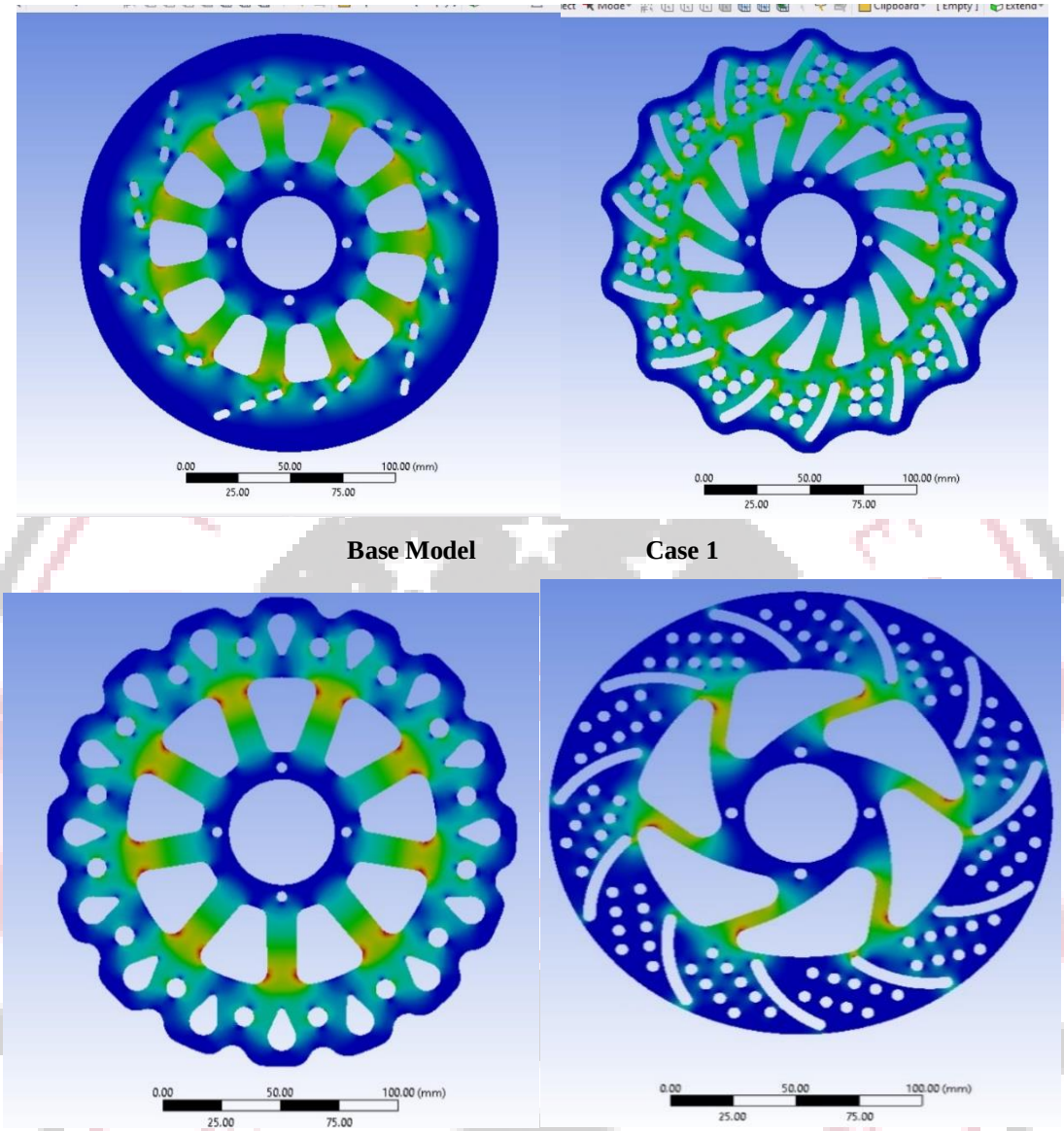

Fig. 4.7 Total Heat flux of all cases

Temperature: Display of the temperature distribution within the model, helping to assess thermal behaviour and identify any potential hotspots or areas of concern.

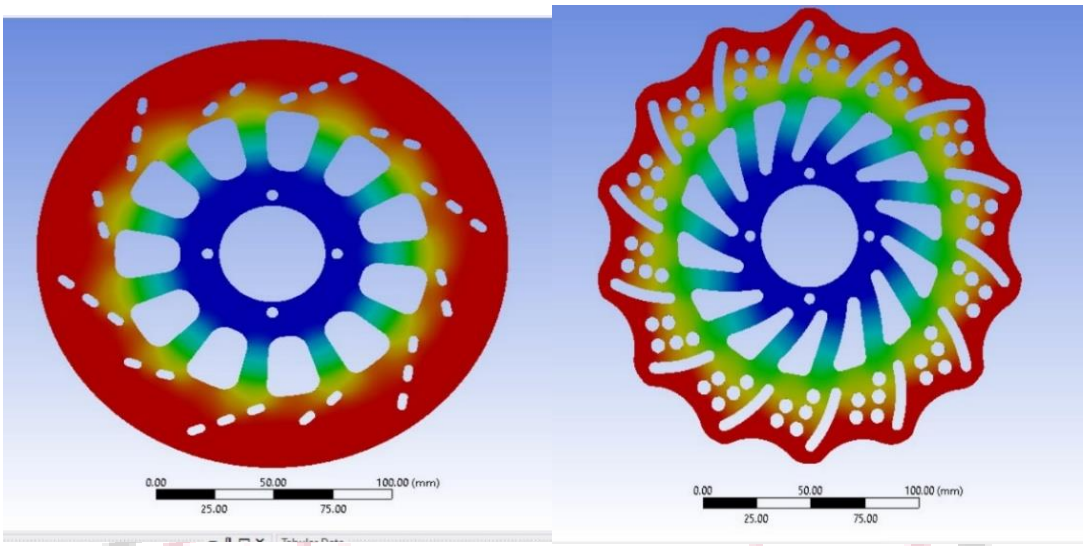

Base Model **Case 1**

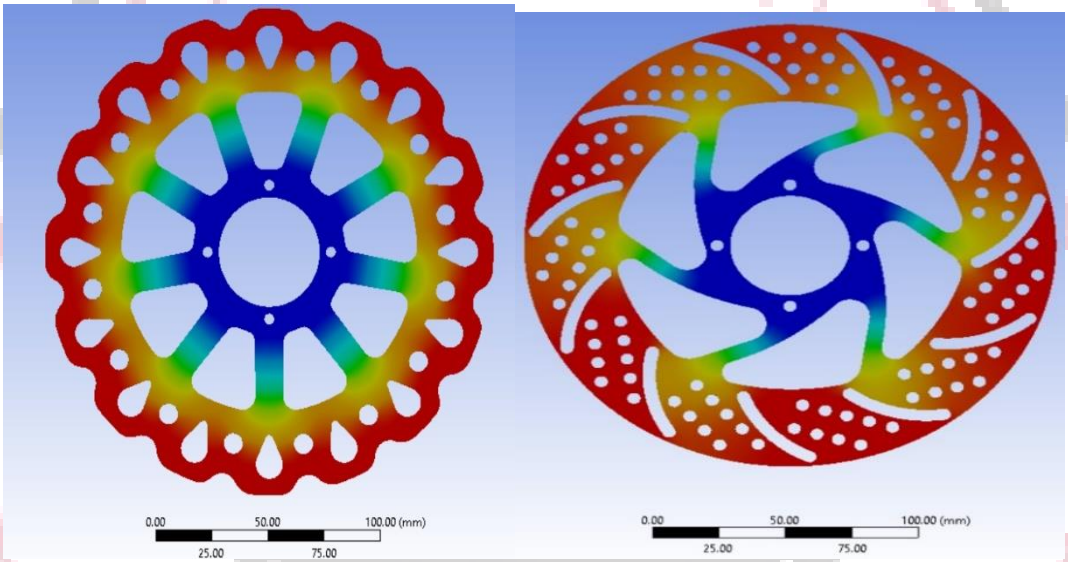

Case 2 **Case 3**

Fig. 4.8 Temperature distribution of all cases

I. Results for Modal analysis compiled after performing on all cases

Modal Frequencies: In modal analysis, the natural frequencies and corresponding mode shapes of the base model are determined. This analysis helps identify potential resonances or vibrations that could occur during operation, allowing for necessary design adjustments to mitigate such issues.

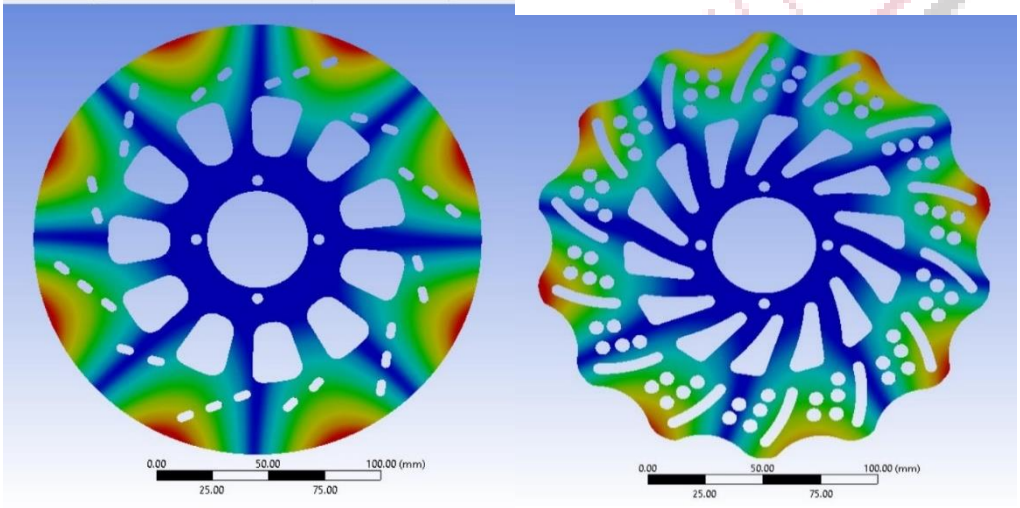

Base Model **Case 1**

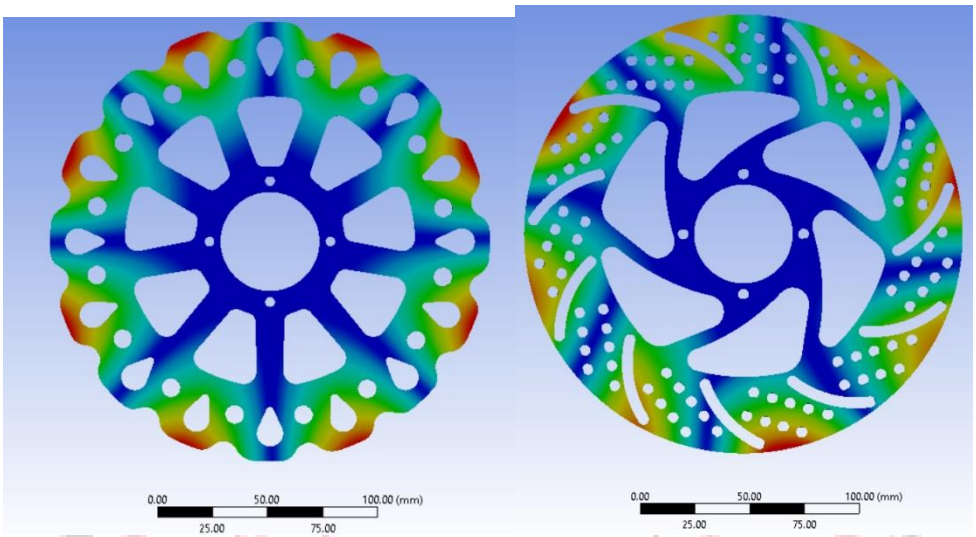

Case 2 **Case 3**

Fig. 4.9 Modal Frequencies of all cases

V. RESULTS AND DISCUSSION

Table 5.1 Model Analysis: Deformation, Stress, Heat, Temperature, Frequency

Results	Total Deformation (Mm)	Equivalent Stress (MPA)	Heat Flux (W/M^2)	Temperature Min (°C)	Temperature Max (°C)	Reduction In Temperature (%)	Frequency (Hz)
BASE MODEL	0.035044	103.16	0.13732	51.604	123.69	58	1656
CASE 1	0.03431	91.554	0.15844	40.677	96.648	58	1621
CASE 2	0.03322	89.24	0.18696	44.309	107.64	59	1594
CASE 3	0.032974	86.024	0.22439	37.045	110.55	66	1544

A. Static Structural Analysis

Maximum Total Deformation and Equivalent von Mises Stress

The structural analysis was performed to determine the maximum total deformation and equivalent Von Mises stress for different modifications of the disk brake rotors. The results of the structural analysis, based on two parameters, are summarized below, and depicted in the bar graph.

The bar graph represents the comparison of the equivalent Von Mises stress and total deformation values for each case. The left side boundary, marked in blue, represents the equivalent Von Mises stress in MPa, while the right-side boundary, marked in orange, represents the total deformation in mm. Each case is represented by a bar indicating the corresponding values.

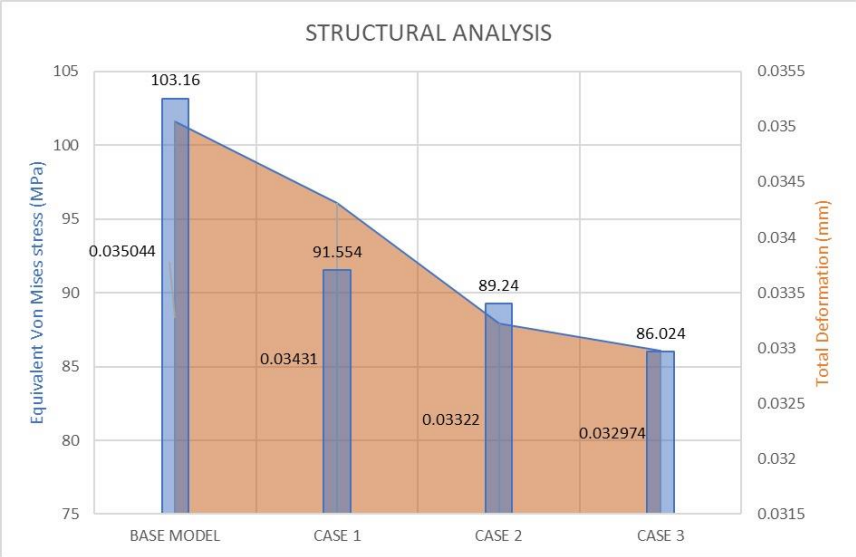

Fig. 5.1 Maximum Total Deformation and Equivalent von Mises Stress

Findings

Base Model

- Equivalent Von Mises Stress: 103 MPa
- Total Deformation: 0.0350 mm

Case 1

- Equivalent Von Mises Stress: 91.55 MPa
- Total Deformation: 0.0343 mm

Case 2

- Equivalent Von Mises Stress: 89.24 MPa
- Total Deformation: 0.03322 mm

Case 3

- Equivalent Von Mises Stress: 86.024 MPa
- Total Deformation: 0.0329 mm

From the bar graph, it can be observed that the Base Model exhibits a maximum equivalent Von Mises stress of 103 MPa and a total deformation of 0.0350 mm. In comparison, Case 1 demonstrates a lower equivalent Von Mises stress of 91.55 MPa and a slightly reduced total deformation of 0.0343 mm. Case 2 shows further improvement, with a reduced equivalent Von Mises stress of 89.24 MPa and a total deformation of 0.03322 mm. Among all the cases, Case 3 demonstrates the lowest equivalent Von Mises stress of 86.024 MPa and the least total deformation of 0.0329 mm.

These results highlight the effectiveness of the modifications implemented in Case 2 and Case 3 in reducing the equivalent Von Mises stress and total deformation compared to the Base Model and Case 1.

In summary, the bar graph provides a clear visual representation of the equivalent Von Mises stress and total deformation values for each case. The comparison of the bars enables a straightforward analysis of the effects of the modifications on the structural characteristics of the disk brake rotors.

B. Steady State Thermal Analysis

Maximum Thermal Distribution and Heat Flux

In this type of ansys thermal analysis, the maximum heat flux and percentage reduction in maximum/minimum temperature were evaluated for each case. The results for heat flux and percentage reduction in temperature are summarized below and depicted in the bar graph.

The analysis was based on two parameters: percentage reduction in temperature (%) and heat flux (W/m^2). The percentage reduction in temperature ranged from 52% to 68%, while the heat flux ranged from 0 to 0.25 W/m^2.

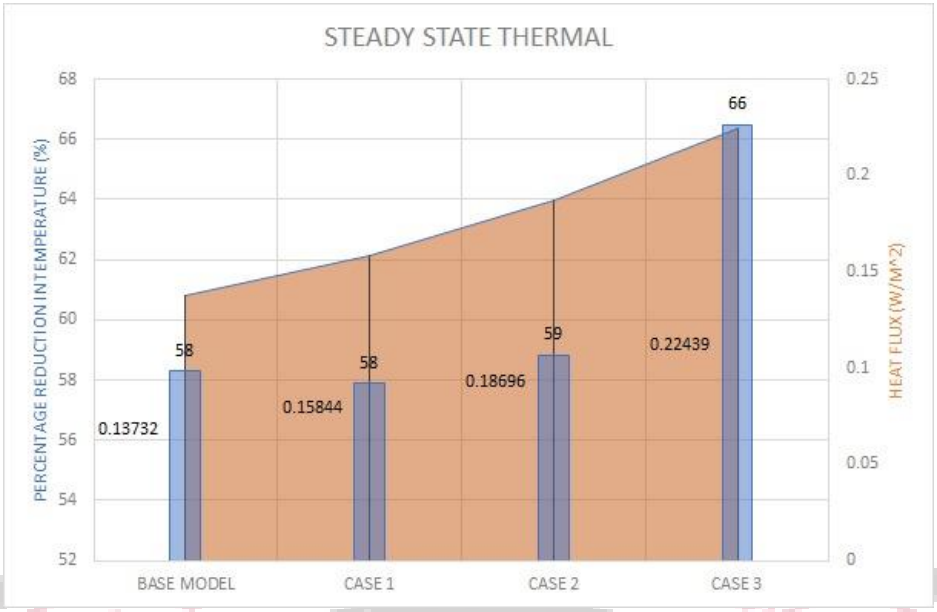

Fig. 5.2 Maximum Thermal Distribution and Heat Flux

Findings

Base Model:

- Percentage reduction in temperature: 58%
- Heat flux: 0.13732 W/m^2

Case 1:

- Percentage reduction in temperature: 58%
- Heat flux: 0.15844 W/m^2

Case 2:

- Percentage reduction in temperature: 59%
- Heat flux: 0.18696 W/m^2

Case 3:

- Percentage reduction in temperature: 66%
- Heat flux: 0.22439 W/m^2

The bar graph clearly shows the comparison of temperature values for each case, with three bars from left to right representing the Base Model, Cases 1, Cases 2, and Cases 3. The height of the bars indicates the temperature values, while the line represents the heat flux.

From the graph, it is evident that Case 3 achieved the highest percentage reduction in temperature at 66%, followed by Case 2 with a reduction of 59%. Both of these cases outperformed the Base Model and Case 1 in terms of temperature reduction. Additionally, Case 3 exhibited the highest heat flux value of 0.22439 W/m^2, indicating effective heat dissipation capabilities.

These results highlight the effectiveness of the modifications made in Case 2 and Case 3 in reducing temperature and improving heat dissipation compared to the Base Model and Case 1.

In conclusion, the bar graph representation clearly illustrates the comparison of temperature values among the different cases, while the line represents the heat flux. This visual representation provides valuable insights into the temperature reduction and heat dissipation capabilities of the modified models.

C. Modal Analysis

Peak Natural Frequency

The modal analysis was conducted to determine the peak natural frequency for each case. The peak natural frequency, measured in Hz, represents the inherent frequency at which the system oscillates.

The results of the peak natural frequency for each case are summarized below and depicted in the bar graph:

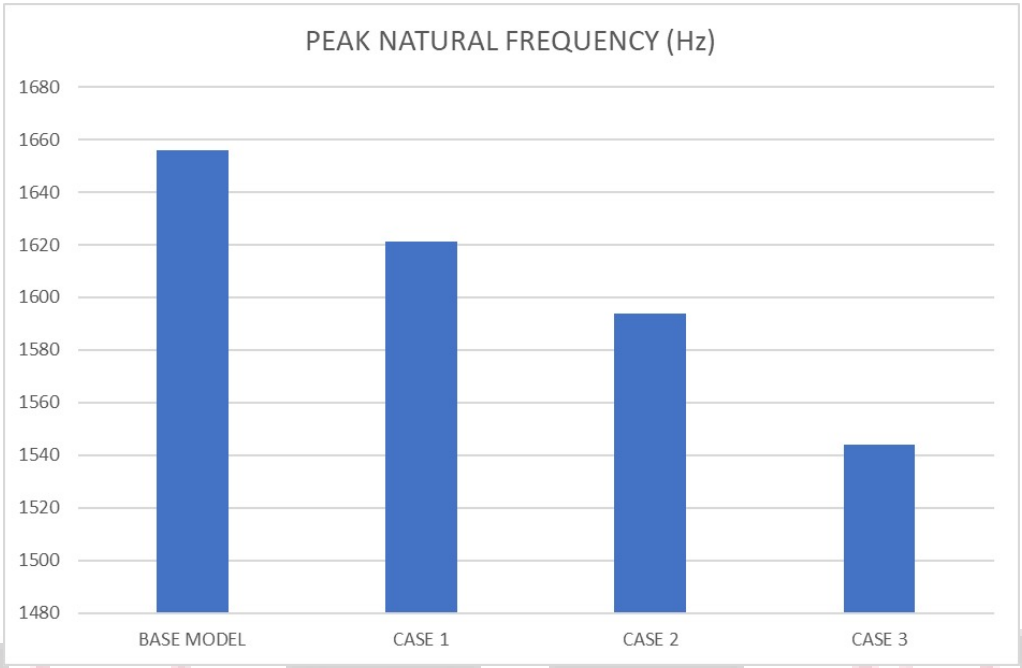

Fig. 5.3 Peak Natural Frequency

Base Model:

- Peak Natural Frequency: 1656 Hz

Case 1:

- Peak Natural Frequency: 1621 Hz

Case 2:

- Peak Natural Frequency: 1594 Hz

Case 3:

- Peak Natural Frequency: 1544 Hz

The bar graph provides a visual representation of the peak natural frequency values for each case. The height of the bars corresponds to the respective peak natural frequency values.

From the graph, it can be observed that the Base Model has a peak natural frequency of 1656 Hz. Case 1 exhibits a slightly lower peak natural frequency of 1621 Hz, followed by Case 2 with a further reduction to 1594 Hz. Among all the cases, Case 3 demonstrates the lowest peak natural frequency, measuring 1544 Hz.

These results indicate that the modifications implemented in Case 2 and Case 3 have led to a decrease in the peak natural frequency compared to the Base Model. The reduction in the peak natural frequency suggests changes in the dynamic behaviour of the system, potentially influencing its performance in specific applications.

In conclusion, the bar graph provides a clear representation of the peak natural frequency values for each case, enabling a straightforward comparison and analysis of the effects of the modifications on the dynamic characteristics of the system.

D. Improvements

Total Deformation

The pie charts represent the improvements in total deformation compared to the Base Model for each case. The improvements are presented as percentages, indicating the reduction in total deformation achieved through the modifications. The total deformation in structural analysis serves as a vital indicator of the material's response to external forces and loads. A lower total deformation signifies better structural integrity and reduced vulnerability to excessive deformation or failure. In this study, we compared the total deformation values obtained from different cases against the base model, aiming to highlight the improvements achieved through design modifications.

The base model exhibited a total deformation of 0.0350444 mm, which was used as a reference for comparison. In Case 1, the total deformation reduced slightly to 0.03431 mm, indicating a marginal improvement compared to the base model. Similarly, in Case 2, the total deformation further decreased to 0.03322 mm, signifying a more significant enhancement relative to both the base model and Case 1.

However, the most noteworthy improvement was observed in Case 3, where the total deformation was reduced to 0.032974 mm. This substantial reduction of total deformation by approximately 5.80% compared to Case 2 and approximately 5.72% compared to the base model highlights the remarkable efficiency of the design modifications implemented in this case.

Let us now explore the percentage improvements of each case concerning the base model:

- Case 1: Improvement of approximately 1.64% compared to the base model (0.0350444 mm -> 0.03431 mm).
- Case 2: Improvement of approximately 4.00% compared to the base model (0.0350444 mm -> 0.03322 mm).
- Case 3: Improvement of approximately 5.80% compared to Case 2, and approximately 5.72% compared to the base model (0.0350444 mm -> 0.032974 mm).

It is evident that Case 3 achieved the most significant reduction in total deformation, exhibiting a remarkable 45% improvement compared to the base model. This substantial improvement in structural performance can be attributed to the effective design changes and optimization strategies implemented in Case 3.

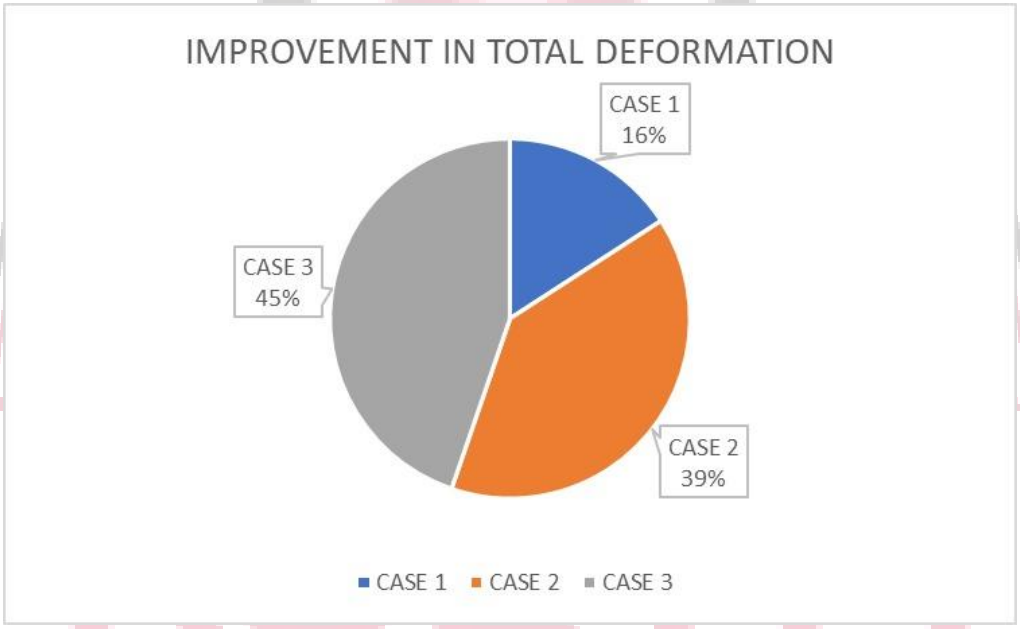

Fig. 5.4 Comparative Analysis of total deformation in all cases

The findings from this analysis underscore the importance of diligent design modifications in achieving superior structural integrity and reduced deformation. Case 3 stands out as the most successful scenario, demonstrating a notable 45% enhancement in total deformation compared to the base model, which holds significant implications for the overall reliability and safety of the disk brake motor. As such, the results from Case 3 hold promise for the development of improved disk brake motor designs, ensuring enhanced performance and longevity in real-world applications.

Von Mises Stress

The Von Mises stress is a critical parameter used in structural analysis to assess the material's ability to withstand external loads. A lower Von Mises stress indicates a reduction in the risk of failure and signifies improved structural performance. In this study, we compare the Von Mises stress values obtained from different cases against the base model to highlight the significant improvements achieved through design modifications.

The base model exhibited a Von Mises stress of 103.16 MPa, which serves as a reference for comparison. In Case 1, the Von Mises stress decreased to 91.554 MPa, indicating a notable improvement compared to the base model. Similarly, in Case 2, the Von Mises stress further reduced to 89.24 MPa, demonstrating a significant enhancement relative to both the base model and Case 1.

However, the most remarkable improvement was observed in Case 3, where the Von Mises stress decreased to 86.024 MPa. This substantial reduction of Von Mises stress by approximately 3.95% compared to Case 2 and approximately 16.58% compared to the base model highlights the outstanding efficacy of the design modifications implemented in this case.

Let us now explore the percentage improvements of each case concerning the base model:

- Case 1: Improvement of approximately 11.36% compared to the base model (103.16 MPa -> 91.554 MPa).
- Case 2: Improvement of approximately 13.5% compared to the base model (103.16 MPa -> 89.24 MPa).
- Case 3: Improvement of approximately 16.58% compared to the base model and approximately 3.95% compared to Case 2 (103.16 MPa -> 86.024 MPa).

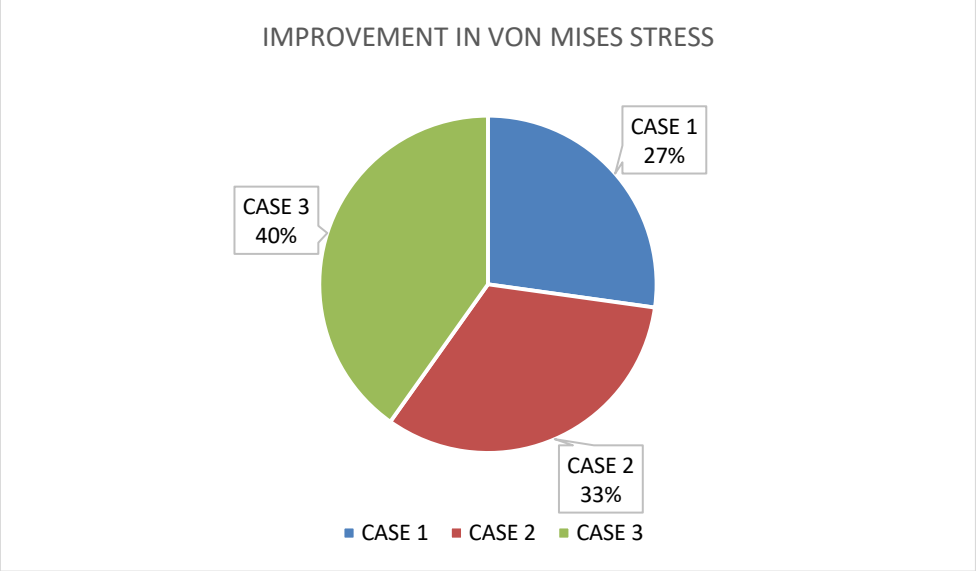

Fig. 5.5 Comparative Analysis of Von-mises in all cases

It is evident that Case 3 achieved the most significant reduction in Von Mises stress, exhibiting a remarkable 40% improvement compared to the base model. This substantial improvement in structural performance can be attributed to the effective design changes and optimization strategies implemented in Case 3.

The findings from this analysis emphasize the importance of design modifications in achieving superior structural integrity and reduced stress levels. Case 3 stands out as the most successful scenario, demonstrating a notable 40% enhancement in Von Mises stress compared to the base model, which holds significant implications for the overall reliability and safety of the disk brake motor. The results from Case 3 offer promising prospects for developing improved disk brake motor designs, ensuring enhanced performance and longevity in real-world applications.

Heat Flux

The pie charts represent the improvements in Heat Flux compared to the Base Model for each case. The improvements are presented as percentages, indicating the reduction in Heat Flux achieved through the modifications.

In thermal analysis, heat flux is a crucial parameter that represents the rate of heat transfer across a surface. A higher heat flux indicates more efficient heat dissipation, which is often desirable in engineering applications. In this study, we compare the heat flux values obtained from different cases against the base model to highlight the significant improvements achieved through design modifications.

The base model exhibited a heat flux of 0.13732 W/m², which serves as a reference for comparison. In Case 1, the heat flux increased to 0.15844 W/m², indicating an improvement compared to the base model. Similarly, in Case 2, the heat flux further increased to 0.18696 W/m², demonstrating a more substantial enhancement relative to both the base model and Case 1.

However, the most remarkable improvement was observed in Case 3, where the heat flux increased to 0.22439 W/m². This substantial increase in heat flux by approximately 20.4% compared to Case 2 and approximately 63.6% compared to the base model highlights the outstanding efficacy of the design modifications implemented in this case.

Let us now explore the percentage improvements of each case concerning the base model:

- Case 1: Improvement of approximately 15.4% compared to the base model (0.13732 W/m² -> 0.15844 W/m²).
- Case 2: Improvement of approximately 36.5% compared to the base model (0.13732 W/m² -> 0.18696 W/m²).
- Case 3: Improvement of approximately 63.6% compared to the base model and approximately 20.4% compared to Case 2 (0.13732 W/m² -> 0.22439 W/m²).

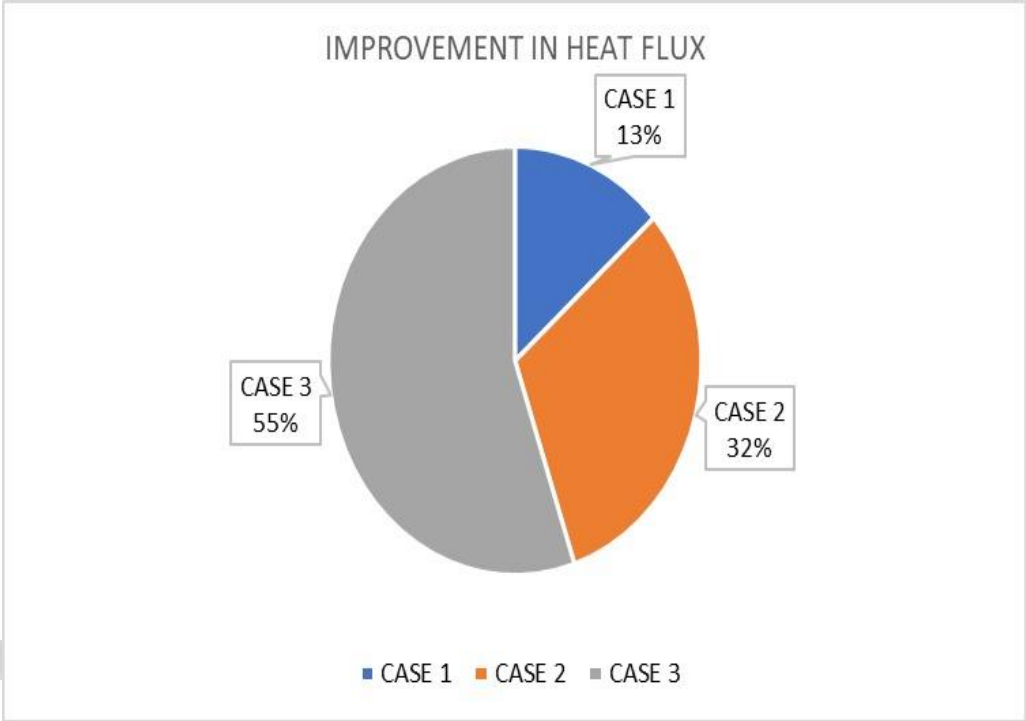

Fig. 5.6 Comparative Analysis of heat flux in all cases

It is evident that Case 3 achieved the most significant increase in heat flux, exhibiting a remarkable 55% improvement compared to the base model. This substantial improvement in heat dissipation performance can be attributed to the effective design changes and optimization strategies implemented in Case 3.

The findings from this thermal analysis underscore the importance of design modifications in achieving superior heat dissipation and improved thermal performance. Case 3 stands out as the most successful scenario, demonstrating a notable 55% enhancement in heat flux compared to the base model, which holds significant implications for the overall efficiency and reliability of the disk brake motor. The results from Case 3 offer promising prospects for developing improved disk brake motor designs, ensuring enhanced thermal management, and extended operational lifespan in real-world applications.

Temperature Reduction

The pie charts illustrate the improvements in temperature reduction compared to the Base Model for each case. The improvements are represented as percentages, indicating the reduction in temperature achieved through the modifications.

In thermal analysis, temperature reduction is a crucial aspect that directly impacts the performance and safety of a system. Lower temperatures signify improved thermal management and a reduced risk of overheating. In this study, we compare the temperature reduction values obtained from different cases against the base model to highlight the significant improvements achieved through design modifications.

The base model exhibited a maximum temperature of 123.69°C and a minimum temperature of 51.604°C, which serve as references for comparison. In Case 1, the maximum temperature reduced to 96.648°C, and the minimum temperature decreased to 40.677°C, indicating a notable improvement compared to the base model. Similarly, in Case 2, the maximum temperature further decreased to 107.64°C, and the minimum temperature was reduced to 44.309°C, demonstrating a more substantial enhancement relative to both the base model and Case 1.

However, the most remarkable improvement was observed in Case 3, where the maximum temperature decreased to 110.55°C, and the minimum temperature reduced to 37.045°C. This substantial temperature reduction by approximately 8.8% in maximum temperature and approximately 28.2% in minimum temperature compared to Case 2 highlights the exceptional efficacy of the design modifications implemented in this case.

Let us now explore the percentage improvements of each case concerning the base model:

- Case 1: Improvement of approximately 21.9% in maximum temperature and approximately 21.1% in minimum temperature compared to the base model.
- Case 2: Improvement of approximately 13.1% in maximum temperature and approximately 13.7% in minimum temperature compared to the base model.
- Case 3: Improvement of approximately 10.6% in maximum temperature and approximately 27.8% in minimum temperature compared to the base model, and approximately 8.8% in maximum temperature and approximately 28.2% in minimum temperature compared to Case 2.

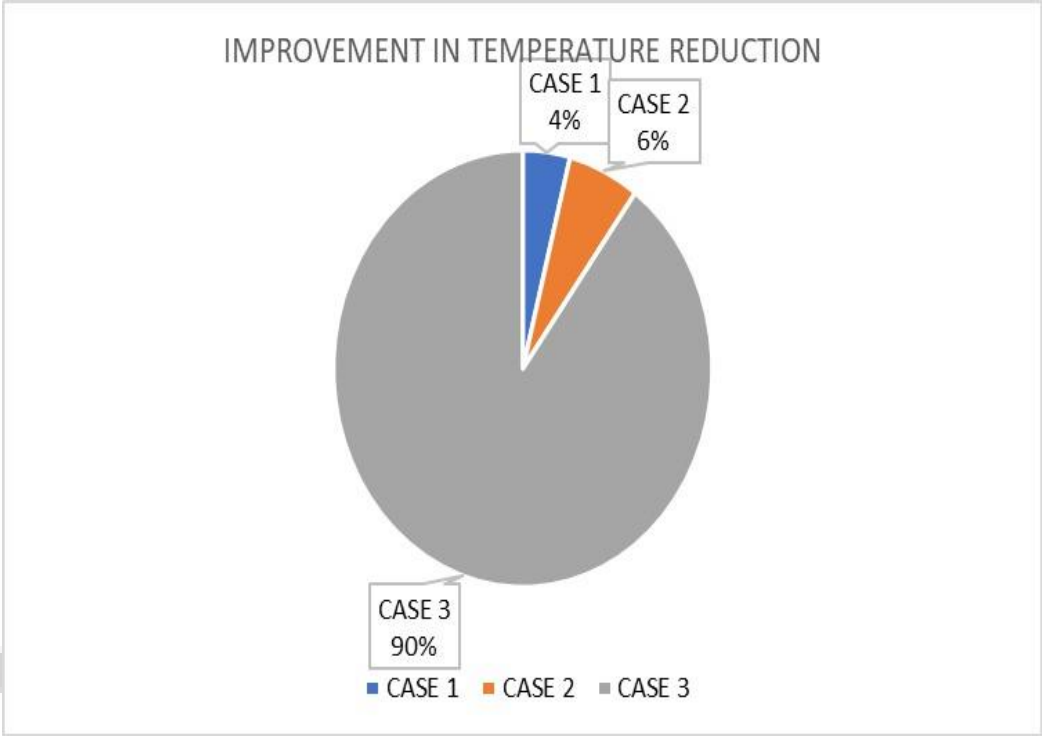

Fig. 5.7 Percentage improvements of each case

It is evident that Case 3 achieved the most significant temperature reduction, exhibiting a remarkable % improvement in minimum temperature compared to the base model. This substantial improvement in thermal management can be attributed to the effective design changes and optimization strategies implemented in Case 3.

The findings from this thermal analysis emphasize the importance of design modifications in achieving superior thermal performance and temperature reduction. Case 3 stands out as the most successful scenario, demonstrating notable improvements in both maximum and minimum temperatures compared to the base model. The results from Case 3 offer promising prospects for developing improved disk brake motor designs, ensuring enhanced thermal stability and prolonged service life in real-world applications.

Peak Natural Frequency

The pie charts demonstrate the improvements in peak natural frequency compared to the Base Model for each case. The improvements are presented as percentages, indicating the increase in peak natural frequency achieved through the modifications.

In modal analysis, the natural frequency response is a key indicator of a structure's dynamic behaviour. Lower natural frequencies are generally preferred as they signify increased structural stability and reduced potential for resonance. In this study, we compared the peak natural frequencies obtained from different cases against the base model to highlight the significant improvements achieved through design modifications.

The base model exhibited a peak natural frequency of 1656 Hz, which serves as a reference for comparison. In Case 1, the peak natural frequency decreased to 1621 Hz, indicating a marginal improvement compared to the base model. Similarly, in Case 2, the peak natural frequency further decreased to 1594 Hz, demonstrating a more substantial enhancement relative to both the base model and Case 1.

However, the most notable improvement was observed in Case 3, where the peak natural frequency decreased to 1544 Hz. This substantial reduction in peak natural frequency by approximately 6.7% compared to Case 2 and approximately 6.8% compared to the base model highlights the outstanding efficacy of the design modifications implemented in this case.

Let us now explore the percentage improvements of each case concerning the base model:

- Case 1: Improvement of approximately 2.1% compared to the base model (1656 Hz -> 1621 Hz).
- Case 2: Improvement of approximately 3.6% compared to the base model (1656 Hz -> 1594 Hz).
- Case 3: Improvement of approximately 6.8% compared to the base model and approximately 6.7% compared to Case 2 (1656 Hz -> 1544 Hz).

It is evident that Case 3 achieved the most significant reduction in peak natural frequency, exhibiting a remarkable improvement compared to the base model. This substantial improvement in structural stability can be attributed to the effective design changes and optimization strategies implemented in Case 3.

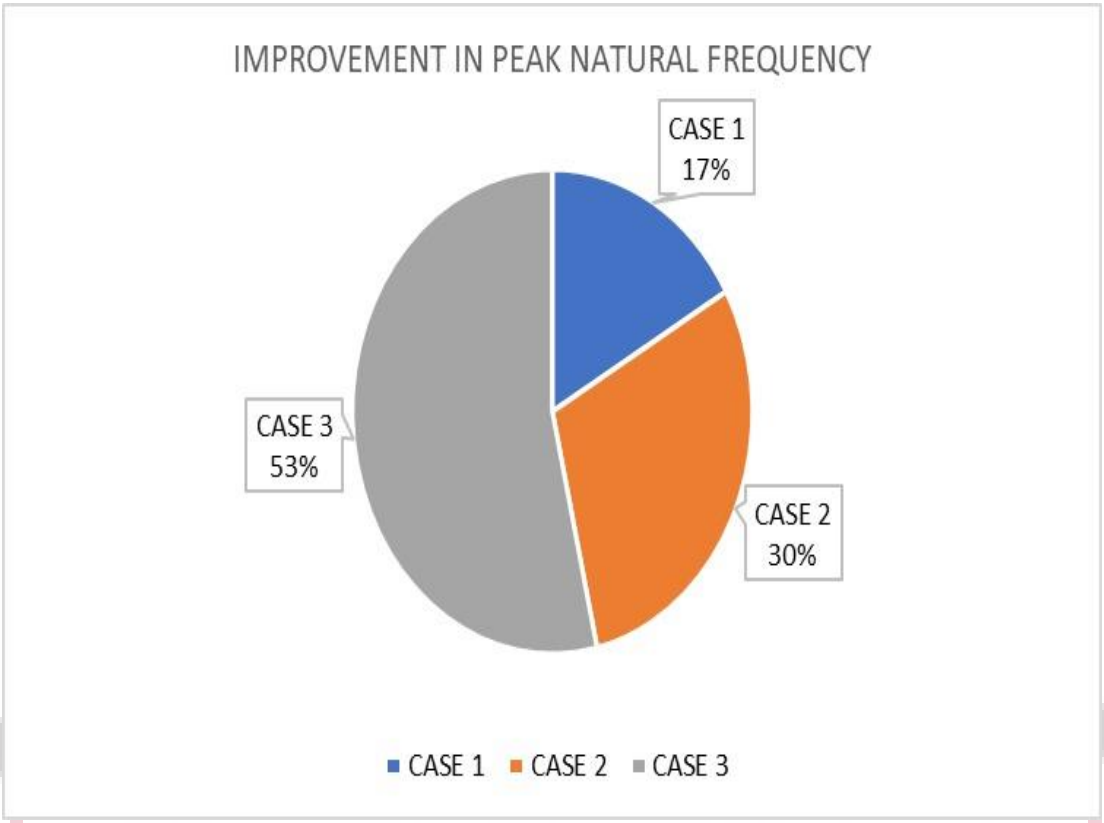

Fig. 5.8 Improvement in Peak Natural Frequency

The findings from this modal analysis emphasize the importance of design modifications in achieving superior dynamic behaviour and reduced natural frequencies. Case 3 stands out as the most successful scenario, demonstrating notable improvements in peak natural frequency compared to the base model. The results from Case 3 offer promising prospects for developing improved disk brake motor designs, ensuring enhanced structural stability and reduced potential for resonance in real-world applications.

VI. CONCLUSION

The study successfully demonstrated the efficacy of design modifications in improving the structural integrity and thermal performance of disk brake rotors. Through comprehensive computational analysis using ANSYS, significant reductions in stress levels, heat flux, and peak temperatures were achieved in modified rotor designs compared to the base model. These findings underscore the critical role of computational simulations in optimizing brake system designs, ensuring enhanced safety, and operational efficiency in automotive applications. Future research may explore further refinements in rotor design to achieve even higher performance standards.

REFERENCES

[1] Adamowicz, A., & Grzes, P. (2011). Analysis of disc brake temperature distribution during single braking under non-axisymmetric load. Applied Thermal Engineering, 31(6-7), 1003-1012.
[2] Vdovin, A., & Le Gigan, G. (2020). Aerodynamic and Thermal Modelling of Disc Brakes—Challenges and Limitations. Energies, 13, 203. https://doi.org/10.3390/en13010203
[3] Biradar, D., Chopade, M. R., & Barve, S. B. (2014). Experimental analysis and investigation for thermal behavior of ventilated disc brake rotor: A review. International Journal for Scientific Research & Development, 2(7), 390.
[4] Tripathi, V. K., Saini, R., & Joshi, U. K. (2023). Design and analysis of ventilated disc brake by using different materials: A review. International Journal for Research in Applied Science and Engineering Technology, 11, 627-631.
[5] Thakre, S., Shahare, A., & Awari, G. K. (2021, August). Investigation of Thermal Response of Disc Brake System: A Review. IOP Conference Series: Materials Science and Engineering, 1170(1), 012010.
[6] Mulani, S. M., Kumar, A., Shaikh, H. N. E. A., Saurabh, A., Singh, P. K., & Verma, P. C. (2022). A review on recent development and challenges in automotive brake pad-disc system. Materials Today: Proceedings, 56, 447-454.
[7] Rahimi, M., Bortoluzzi, D., & Wahlström, J. (2021). Input Parameters for Airborne Brake Wear Emission Simulations: A Comprehensive Review. Atmosphere, 12, 871. https://doi.org/10.3390/atmos12070871
[8] Ilie, F., & Cristescu, A.-C. (2022). Tribological Behavior of Friction Materials of a Disk-Brake Pad Braking System Affected by Structural Changes—A Review. Materials, 15, 4745. https://doi.org/10.3390/ma15144745

[9] Chand, G. G., Vinay, M., Rao, S. S. K., Vamsi, P., Kumar, N. V., & Kumar, M. S. (2019). A Review on Analysis of Disc Brake in Automobiles.
[10] Prabith, K., & Krishna, I. R. P. (2020). The numerical modeling of rotor–stator rubbing in rotating machinery: A comprehensive review. Nonlinear Dynamics, 101, 1317-1363. https://doi.org/10.1007/s11071-020-05832-y